NeuroImage 246 (2022) 118756

Contents lists available at ScienceDirect

NeuroImage

journal homepage: www.elsevier.com/locate/neuroimage

Distinct neural-behavioral correspondence within face processing and attention networks for the composite face effect

Changming Chen [a], Yixue Lou [b,d], Hong Li [c,d,**], Jiajin Yuan [d,*], Jiemin Yang [d], Heather Winskel [e], Shaozheng Qin [f,g]

[a] School of Education, Chongqing Normal University, Chongqing 401331, China
[b] Department of Psychology, Faculty of Education and Psychology, University of Jyvaskyla, Jyväskylä 40014, Finland
[c] Centre for Studies of Psychological Applications, Guangdong Key Laboratory of Mental Health and Cognitive Science, Key Laboratory of Brain Cognition and Educational Science, Ministry of Education, School of Psychology, South China Normal University, Guangzhou 510631, Guangdong, China
[d] Institute for Brain and Psychological Sciences, Sichuan Normal University, Chengdu 610054, Sichuan, China
[e] Psychology, James Cook University, Singapore Campus, 387380, Singapore
[f] State Key Laboratory of Cognitive Neuroscience and Learning & IDG/McGovern Institute for Brain Research, Beijing Normal University, Beijing 100875, China
[g] Chinese Institute for Brain Research, Beijing, China

ARTICLE INFO

Keywords:
Face recognition
Functional magnetic resonance imaging
Representational similarity analysis
Insula
Fusiform gyrus
Composite face effect

ABSTRACT

The composite face effect (CFE) is recognized as a hallmark for holistic face processing, but our knowledge remains sparse about its cognitive and neural loci. Using functional magnetic resonance imaging with independent localizer and complete composite face task, we here investigated its neural-behavioral correspondence within face processing and attention networks. Complementing classical comparisons, we adopted a dimensional reduction approach to explore the core cognitive constructs of the behavioral CFE measurement. Our univariate analyses found an alignment effect in regions associated with both the extended face processing network and attention networks. Further representational similarity analyses based on Euclidian distances among all experimental conditions were used to identify cortical regions with reliable neural-behavioral correspondences. Multidimensional scaling and hierarchical clustering analyses for neural-behavioral correspondence data revealed two principal components underlying the behavioral CFE effect, which fit best to the neural responses in the bilateral insula and medial frontal gyrus. These findings highlight the distinct neurocognitive contributions of both face processing and attentional networks to the behavioral CFE outcome, which bridge the gaps between face recognition and attentional control models.

1. Introduction

The concept of holistic processing is central to face recognition research (Richler et al., 2011). It is generally believed that faces are perceived as indecomposable wholes rather than as a collection of separate parts (Richler et al., 2012; Rossion, 2013; Tanaka & Farah, 1993). Holistic processing can be characterized by multiple different phenomena (Maurer et al., 2002; Richler et al., 2012), such as the “face inversion effect” where people recognize upright faces better than inverted faces (Yin, 1969), and the “whole-part effect" where the recognition of a face part is better when presented in a whole face compared to when presented in isolation (Tanaka and Farah, 1993). In the current study we investigate the composite face effect (CFE) which has gained growing interest and provides one of the most powerful pieces of evidence for holistic processing (Hole, 1994; Rossion, 2013; Young et al., 1987). Unlike the whole-part effect which emphasizes the facilitation effect of holistic processing on immediate and long-term face memories, the CFE effect emphasizes holistic attention (Richler et al., 2012; Tanaka and Simonyi, 2016). It describes a difficulty in selective processing of a target face part (e.g. the top half) while ignoring the remaining part of a face (e.g. the bottom half), probably due to the interference of the latter (Richler et al., 2012).

The CFE effect is named after the composite face paradigm which has been refined over the past three decades (Gauthier and Bukach, 2007; Hole, 1994; Young et al., 1987). In the original version of this paradigm the top halves are either identical or different but the bottom halves are always different, and the CFE is indexed by an alignment effect in trials with identical tops (Rossion, 2013; Young et al., 1987): participants are prone to errors when matching two identical target halves that are aligned with different irrelevant halves, but show high performance

* Institute of Brain and Psychological Sciences, Sichuan Normal University, Chengdu 610066, China
** School of Psychology, South China Normal University, Guangzhou 510631, China
E-mail addresses: lihong_psych@m.scnu.edu.cn (H. Li), yuanjiajin168@sicnu.edu.cn, yuanjiajin168@126.com (J. Yuan).

https://doi.org/10.1016/j.neuroimage.2021.118756.
Received 11 August 2021; Received in revised form 14 November 2021; Accepted 22 November 2021
Available online 27 November 2021.

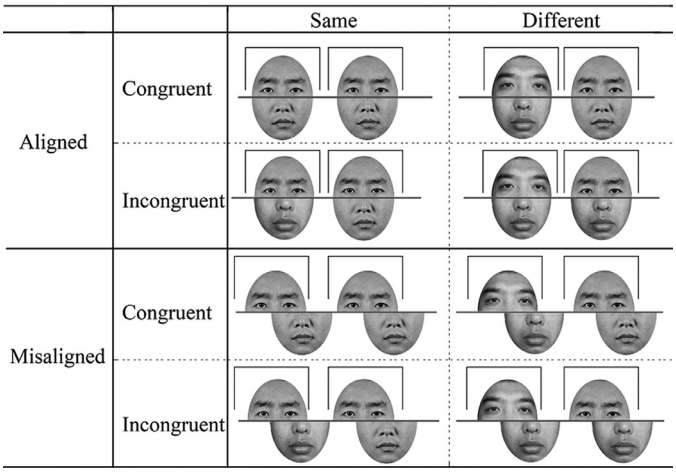

Fig. 1. Design and example stimuli of the complete composite face paradigm (CCP). Participants are asked to match the top halves of two composite faces indicated by the brackets. In the congruent condition the top and bottom halves are either both identical or both different, whereas in the incongruent condition they are identical at one location but different in the other location. The top and bottom halves are either aligned or misaligned. Portrait rights were consented by the persons depicted.

when the target and irrelevant halves are misaligned. To minimize the confound of response bias, an additional manipulation of "congruency" is later included in research articles ("complete composite paradigm", CCP, see Fig. 1, Gauthier and Bukach, 2007). In the "congruent" trials the top and bottom halves are either both identical or both different, whereas in the "incongruent" trials the two parts are identical in one location (e.g., the top) but different in the other (e.g., the bottom). Researchers have repeatedly observed the modulation of congruency and spatial alignment: the response is facilitated (higher discrimination index and shorter reaction time) in the "congruent" than the "incongruent" trials when faces are aligned, while this congruency effect is reduced or disappears when faces are misaligned (Cheung et al., 2008; Richler and Gauthier, 2014).

Since its introduction, the CFE effect has emerged as one of the tried-and-true measures of holistic processing (Richler and Gauthier, 2013; Rossion, 2013; Young et al., 1987). It has been intensively investigated, stimulating ongoing interests and discussions about the nature of holistic processing, such as its domain-specificity (Chua and Gauthier, 2020; Gauthier and Tarr, 2002; Rossion, 2013; Bauser et al., 2011; Zhao et al., 2015, 2016), development (Grand et al., 2004; Ventura et al., 2018), association with face recognition ability (significant in DeGutis et al., 2013; Richler et al., 2011; Wang et al., 2012; but null in Konar et al., 2010; Rezlescu et al., 2017; Zhao et al., 2014) and its link to perceptual expertise (Gauthier and Bukach, 2007; Gauthier and Tarr, 1997; Zhao et al., 2015). It has also become a paradigm with much potential in delineating emotion recognition (Calder et al., 2000; Xie and Zhang, 2016), social cognition (Chen et al., 2018; Todorov et al., 2010), modelling of face processing (Dailey and Cottrell, 1999; Fitousi, 2013), aberrant face perception in clinical populations such as autism (Gauthier et al., 2009) and prosopagnosia (significant in Avidan et al., 2011; Busigny et al., 2010; Liu and Behrmann, 2014; Ramon et al., 2010, but null in Biotti et al., 2017; Le Grand et al., 2006; Susilo et al., 2010), contributing substantially to our understanding of face and object recognition (Murphy et al., 2017). But along with the popularity of the CFE effect is its unresolved neurocognitive operations, especially how it is affected by perceptual and attention processes.

According to the template hypothesis (Jacques and Rossion, 2009; Rossion, 2013; Tanaka and Farah, 1993), face recognition relies heavily on simultaneous perceptual integration of separate features which fuses facial parts into a quintessential whole (Gestalt), it is realized by a template-matching process guided by an inherently holistic internal representation (page 145, Rossion, 2013). In some articles the CFE is argued as a perceptual illusion (page 140, Rossion, 2013) unique in upright faces (McKone et al., 2013), and roles of factors like object-based attention or decisional components are rejected as "they are unable to account for the CFE effect" (page 191, Rossion, 2013; McKone et al., 2013). In terms of its dynamics, the template hypothesis proposes that the CFE is initiated by perpetual integration from early onset (Jacques and Rossion, 2009; Rossion, 2013) implemented in face-sensitive areas including the fusiform and occipital face areas along the ventral occipito-temporal cortex (Schiltz et al., 2010; Schiltz and Rossion, 2006). Consistent with this, fMRI studies with block-design (Schiltz and Rossion, 2006) and event-related design (Schiltz et al., 2010) find neural adaptations in the bilateral middle fusiform gyrus and inferior occipital gyrus when identical top halves were aligned with different bottom halves than the condition where identical tops were aligned with identical bottoms, but not in misaligned or inverted faces. Electrophysiological studies observed an increase in the N170 component in the occipito-temporal cortex following changes of identity in the top and bottom halves (Kuefner et al., 2010; Von Der Heide et al., 2018). The within-network connectivity in the rFFA correlates negatively with the composite-face effect, and the functional connectivity between rFFA and bilateral posterior superior temporal sulcus is also negatively linked to the behavioral CFE effect (Li et al., 2019). The CFE effect is reduced following transcranial direct current stimulation (tDCS) over the occipito-temporal cortex (Yang et al., 2014), or lesions in the anterior region of the right temporal lobe (Busigny et al., 2014). However, it is worth noting that face processing in the OFA is more part-based (Liu et al., 2010; Zhang et al., 2015) and there is coexistence of both part-based and whole-based representation of the FFA (Harris and Aguirre, 2008, 2010; Liu et al., 2010). Differences in neural response between aligned and misaligned composite faces are also reported in regions including the lateral occipital complex, parahippocampal gyrus (Foster et al., 2015) and even the prefrontal cortex (Schiltz et al., 2010). Mixed pictures are suggested about the neural correlates of the CFE effect, within and outside the face network.

In parallel, the CFE effect is also observed in non-face objects such as greebles (Gauthier and Tarr, 1997; Gauthier et al., 1998), visual words (Wong et al., 2012) or even inverted faces (Susilo et al., 2013). The expertise hypothesis proposes that holistic face processing arises from a learned strategy of attending to all parts due to substantial experience in face individuation (Gauthier and Bukach, 2007; Gauthier and Tarr, 1997; Gauthier et al., 1998). Specifically, because "individuation in everyday life encourages attention to all parts" (Chua et al., 2014), the attentional strategy to full face becomes automatic and cannot be easily "turned off" after extensive experience in face individuation. The CFE effect then arises as a failure of selective attention because of the "inflexibility in attentional weightings on facial parts" (page 4, Richler et al., 2012). According to this view, holistic processing can be observed both in faces and non-face objects given a massive amount of individuation experience (Gauthier and Tarr, 1997; Wong et al., 2012). In line with this, individuation experience attending to the whole face particularly the diagnostic features lead to holistic processing (Chua et al., 2014; Chua et al., 2015) and the level of experience in individuating objects of a category determines the extent of holistic processing in new objects of that category (Chua and Gauthier, 2020). fMRI studies also show neural correlates of expertise in FFA. There is, for instance, higher FFA response to objects of expertise in experts than novices (Gauthier et al., 2000), as well as correlation between FFA response to the expertise objects and behavioral indices of holistic processing of those objects (Gauthier and Tarr, 2002; Ross et al., 2018; Wong et al., 2009).

Nevertheless, the CFE effect is also observed in non-face object without expertise such as line patterns (Zhao et al., 2015). The shape-based account proposes there might be two routes for the holistic processing (Foster et al., 2021; Zhao et al., 2016): it can arise either via a top-down

expertise route or via a bottom-up route relying merely on Gestalt information. This account suggests holistic processing is tuned to facial shape information as "shape information alone is sufficient to elicit the composite face effect" regardless of its origins from innate face template or automatized attention (Zhao et al., 2016). Recruiting the complete composite paradigm, Foster et al. (2021) observed higher activities to holistic versus part-based processing in areas within the face-responsive network (e.g. FFA2) and areas outside such as the lateral occipital complex, transverse occipital sulcus, retrosplenial cortex and the parahippocampal place area.

An additional hypothesis (Fitousi, 2015, 2016) also agrees with the domain-generality of the CFE effect, but surmises CFE reflects a general attentional strategy akin to object-based attention. Different from the aforementioned "integrating" hypotheses, Fitousi and colleagues propose the CFE effect does not necessitate the integration of information in the top and bottom face halves, but could be due to differences in the relative discriminability between them (Fitousi, 2016; Fitousi and Algom, 2006), or due to decisional factors across conditions (Fitousi, 2016). The reduction in the congruity composite effect with misalignment is likely due a similar disruption of objecthood (Fitousi, 2015) as in object-based attention all constituent features or parts can be activated once an object has been selected. Computational modelling based on multidimensional signal detection theory suggests the CFE is affected by not only perceptual, but also attentional and decisional components (Richler et al., 2009; Richler et al., 2008). Analysis of theoretical ex-Gaussian parameters of RT distributions (Fitousi, 2020) also reveals that the CFE effect is generated by pure changes in the exponential component of the ex-Gaussian distribution, suggesting the involvement of attentional and working memory processes in the composite face effect regardless of partial and complete designs. Other study also revealed behavioral evidence for violations of perceptual separability, decisional separability, and believed that "holistic processing could very well be a product of both perceptual and decisional influences even when overt response is not required" (Von Der Heide et al., 2018). The involvement of these loci can be further supported by neuroimaging observation that the change of identity of the top of the composite face is associated with a signal increase at the later decisional P3b component and the lateralized readiness potential (LRP) (Kuefner et al., 2010).

Taken together, these studies generally agree on the involvement of a perceptual component in the CFE effect, but hold different views about the role of other cognitive processes such as attentional, decisional or working memory. It is theoretically interesting to admit and elaborate on the contribution of perceptual components to the CFE effect, but increasing evidence shows clearly that the composite face effect is to some degree modulated by other sources of influence (Liu et al., 2020; Murphy et al., 2017; Von Der Heide et al., 2018). Therefore, to get a fair understanding of the CFE effect, we believe it is of equal importance to adopt a more inclusive approach, targeting the debated cognitive processes directly and weighing their neural substantiation in the composite face task. However, till now the majority of existent studies emphasize the role of face regions, though a few studies have inspected regions beyond the face network their interests are still restricted to regions within the ventral or dorsal perceptual streams (Foster et al., 2021), the neural operations beyond remains also largely unknown.

Meanwhile, methodologically most of the previous studies examined the neural correlates of the CFE via top-down approaches (Foster et al., 2021; Schiltz et al., 2010; Schiltz and Rossion, 2006), using univariate statistical parametric mapping methods contrasting conditions critical for a theoretical inference. While informative, these approaches are subject to limitations in the ability to explore representation of multidimensional data (Popal et al., 2020) and may overlook valuable information in condition-rich designs like the complete composite paradigm. Sophisticated multivariate, model-free techniques such as representational similarity analysis (RSA, Kriegeskorte et al., 2006; Kriegeskorte et al., 2008) can make the enrichment. The RSA uses distance measures such as response-pattern dissimilarities (1 - correlation) or the Euclidean distance among the experimental conditions (Kriegeskorte et al., 2008) to characterize the high-order representational space. Combining with second-level reduction techniques such as multidimensional scaling, it can reveal the relationship among multiple experimental conditions/manipulations and visualize the internal structure of mental operations (Kriegeskorte et al., 2008). It can be used to fit neural activities in cortical regions to behavioral profiles or computational models (Arbula et al., 2021; Qin et al., 2014). During the past decade, the RSA has been widely used to explore the response similarity between species (Kriegeskorte et al., 2008), stages of cognitive processing (Tzagarakis et al., 2009), cortical regions and modalities of brain-activity measurement (Benjaminsson et al., 2010; Kriegeskorte et al., 2008), being particularly beneficial in condition-rich experimental design (Kriegeskorte et al., 2008).

Given these theoretical and methodological concerns, the current study investigated the roles of the face-processing network and the attentional network in the CFE, with especial interest in which networks demonstrate satisfactory neural-behavioral fitting. We conducted magnetic resonance imaging when participants received the complete composite task, and independent face localizer scanning to define these two networks. The attentional interference network was defined by the Eriksen Flanker task—a popular paradigm measuring attentional interference (Eriksen and Eriksen, 1974), and the face processing network was identified by the one-back recognition task involving face and non-face stimuli. Complementing the conventional univariate analysis, we recruited the representational similarity analysis to assess the relationship between behavioral and neural activity patterns. Based on the Euclidian distances among all eight conditions, we conducted multidimensional scaling analysis and hierarchical clustering to explore the principal components underlying the experimental conditions and to visualize the respectively behavioral and neural representational (dis)similarity structure. We then explored behavioral-neural correspondence via ROI-based analyses and whole-brain searchlight analysis, based on Spearman's-rank correlation between the dissimilarity matrices. The results are expected to shed light on the implementation of perceptual and attentional processes in the CFE effect, and contribute to the neurocognitive framework of face processing.

2. Methods

The study was approved by the Brain Imaging Center Institutional Review Board of Southwest University, China. Informed consent was obtained in written form from all participants prior to the study.

2.1. Participants

Twenty-two undergraduate or graduate students (13 females, 21.451.37 years old) from a university in mainland China participated in all the tasks and MRI scanning as detailed below (also see supplementary materials). Satisfactory statistical power was expected in the current design as a previous study reported a sample size of 15 participants could detect acceptable effect size both in behavioral and fMRI measurements using the same complete composite face paradigm (Foster et al., 2021). None of the participants had a history of neurological or psychiatric illness, or reported difficulty in recognizing faces and everyday objects. They were right-handed and had normal or corrected-to-normal visual ability. They scored 59.36 ± 8.91 (range: 41–72, total score:72) in the Chinese version of the Cambridge Face Memory Test (McKone et al., 2012) and 45.86 ± 7.09 (range: 35–65, total score:72) in the Cambridge Car Memory Test (Dennett et al., 2012).

2.2. The experimental design

The fMRI scanning was carried out in two sessions. The first session consisted of high-resolution structural imaging, face-network localizer and Eriksen Flanker localizer tasks, as well as rest-state and DTI scanning

(not reported here). The second session was carried out later within three days, where participants received 4 runs of functional imaging when performing the complete composite face task. Stimuli used in the second session were not seen in the first session.

2.3. Tasks and materials

Face-network Functional Localizer Task: The localizer scanning consisted of 3 runs. Each run lasted for 5 min 12 secs and presented the following five categories in blocks: faces, houses, words, cars and scrambled words. Participants were asked to perform a one-back task detecting stimulus repetition, where the occurrence of repetition was no more than twice in each block. All the blocks were 12-s long and sandwiched by 8-s fixations. In each block 10 stimuli were presented sequentially: each was presented for 600 ms and followed by a 600 ms fixation. In total, there were 9 blocks for each category. The order of the categories was counterbalanced across runs and participants.

Eriksen Flanker Task: In this task, participants were asked to judge the orientation of the central arrow, which was flanked by two stimuli on each side. The flanker stimuli were either arrows orienting to the same direction (congruent trials), or arrows orienting to the opposite direction to the central arrows (incongruent trials) or stars (neutral trials). These three trial types were interspersed randomly across two runs. Each run lasted for 6 min 20 s, and contained 40 trials for each trial type. The trials from the three conditions showed up in a pseudo-random way such that there were no more than 3 consecutive trials with the same response. In each trial, the arrow image was presented for 500 ms, and followed by a fixation for either 1500 ms or 3500 ms.

Complete Composite Face Task: A total of 16 grayscale young adult Chinese faces (8 females) were used to create the composite faces. All the raw faces had neutral expressions, were the same age, grayscale, and equalized in physical properties like luminance and contrast. External features such as hair, eye glasses, and earrings were removed. There were no distinguishing features (moles or scars) that could facilitate feature-based face recognition. To generate the composites, all faces were horizontally divided into two halves in the middle, the top half of each face was aligned with the bottom half of two others of the same gender. Composites with unsatisfactory face configuration were discarded according to the following criteria: misalignment in the contours of the top and lower halves, misalignment between the nose from the center of the mouth, irregular ratio of upper lip height to mouth width (< 0.3 or > 0.7) based on a norm of Chinese population (Wang et al., 2019). Thirty-two aligned composite faces were constructed following this procedure. Misaligned faces were then generated from these composites by shifting the bottom half 70 pixels rightward and inserting a horizontal red line (3 pixels) at the conjunction of two halves. We also added a white bracket over the head of all pictures to signify the target location. All stimuli were presented at the center of the screen at a distance of 100 cm. All the aligned composites were 130×170 pixels (visual angle: $1.76^o \times 2.29^o$), and the misaligned composites were 200×170 pixels (visual angle: $2.70^o \times 2.29^o$). Participants were asked to match the top halves of the two composite faces (see Fig. 1b). There were 4 runs of scanning. Each run lasted for 9 min 56 s and contained 144 trials, with 18 trials in each of the 8 conditions (aligned/misaligned × congruent/incongruent × same/different response). At the beginning of each run, a white bracket showed up in the upper half of the screen to notify participants that the top halves should be compared. Each trial began with a study face (300 ms), then a mask (120 ms), the cue bracket (280 ms), and finally a test face (300 ms). Between each two trials there was a fixation for either 1000, 3000 or 5000 ms.

2.4. Imaging parameters

Whole-brain anatomical and functional images were collected using a 12-channel head coil on a 3.0-T Siemens Trio MRI scanner (Siemens Medical, Erlangen, Germany). The functional images were collected with a T2*-sensitive Echo Planar Imaging sequence (Sequence = epfid2d1.64), with equal parameters for all three tasks: TR/TE = 2000 ms/30 ms, flip angle = 90°, number of slices = 32, slice thickness = 3.0 mm, slice gap = 1.00 mm, matrix = 64 × 64, voxel size = 3.4375 × 3.4375 × 3 mm^3. The whole-brain High-resolution T1-weighted anatomical images were collected using a magnetization-prepared rapid gradient echo (MPRAGE) sequence, with parameters as below: TR/TE/TI = 1900 ms / 2.52 ms / 900 ms, flip angle = 9°, number of slices = 176, slice thickness = 1.0 mm, matrix = 256 × 256, voxel size = 1 × 1 × 1 mm^3.

2.5. Image preprocessing and GLM analysis

Data were analyzed using the Analysis of Functional NeuroImages software (AFNI, http://afni.nimh.nih.gov/afni/) and in-house Matlab codes (Mathworks, MA). Functional images in all three tasks were preprocessed following the same pipeline. The first four volumes of each run were discarded for stabilization of magnetic resonance signal. The remaining were corrected for slice acquisition timing, and spatially realigned to correct for head movement. Data for all the tasks were aligned to the first volume of the face network localizer, and then scaled against the mean value of each run. In the univariate analysis, the scaled time courses were smoothed by a Gaussian Kernel of 6 mm FWHM. Deconvolution analyses were then conducted to estimate the regression beta values for conditions in each task based on GLM theory. The basis function for the 5 categories in face network localizer task was BOX(1,12), and the basic function for predictors in other two tasks was GAMA. Six parameters of head movement were also included in the regression model. The beta value maps were then normalized to the Talairach space and resampled into resolution of 3 × 3 × 3 mm^3.

2.6. ROI analysis

Definition of regions of interest ROIs in the face network were identified by contrasting BOLD response for faces versus houses and cars, each ROI was extracted at the individual level at the height threshold of $p < 0.05$. ROIs in the Eriksen Flanker Task were regions with higher BOLD response to the “incongruent” than the “congruent” trials based on the results of group analysis, corrected by FDR method at $p < 0.05$.

Similar to other studies using the complete composite face paradigm, the trials were grouped into four categories at the combination of alignment and congruency, collapsing top-same and top-different trials in each category to obtain the discrimination index and mean reaction time. However, as the top-same and top-different trials contribute differentially to the behavioral composite face effect and share distinct neural representations, it is recommended that separate analysis of these two types of trials may help clarify their roles in measuring holistic processing (Foster et al., 2021). Therefore, we grouped the trials into 8 conditions at the combination of the three factors: alignment (aligned, misaligned) × congruency (congruent, incongruent) × response type (same, different) and first ran univariate analyses on the BOLD signal estimated by general linear model.

Additionally, we ran a representational similarity analysis (RSA) to quantitatively explore how well neural responses in regions of face processing and attentional interference networks fit the behavioral results. In each region, we constructed the activity-pattern dissimilarity matrix of the 8 conditions based on the Euclidean distance, and visualize the similarity structure of neural activities of the conditions combining multidimensional scaling with hierarchical clustering. The reference behavior-based dissimilarity matrix was estimated in the same way based on the inverse efficiency score (IES = RT/ACC), which takes the joint contribution of accuracy and reaction time into consideration. The behavioral-neural correspondence in each region of interest was then estimated by Spearman’s rank correlation between the upper triangular elements of the two matrices. The neural-behavioral correspondence in a region was assessed by a random permutation simulation (10000 times),

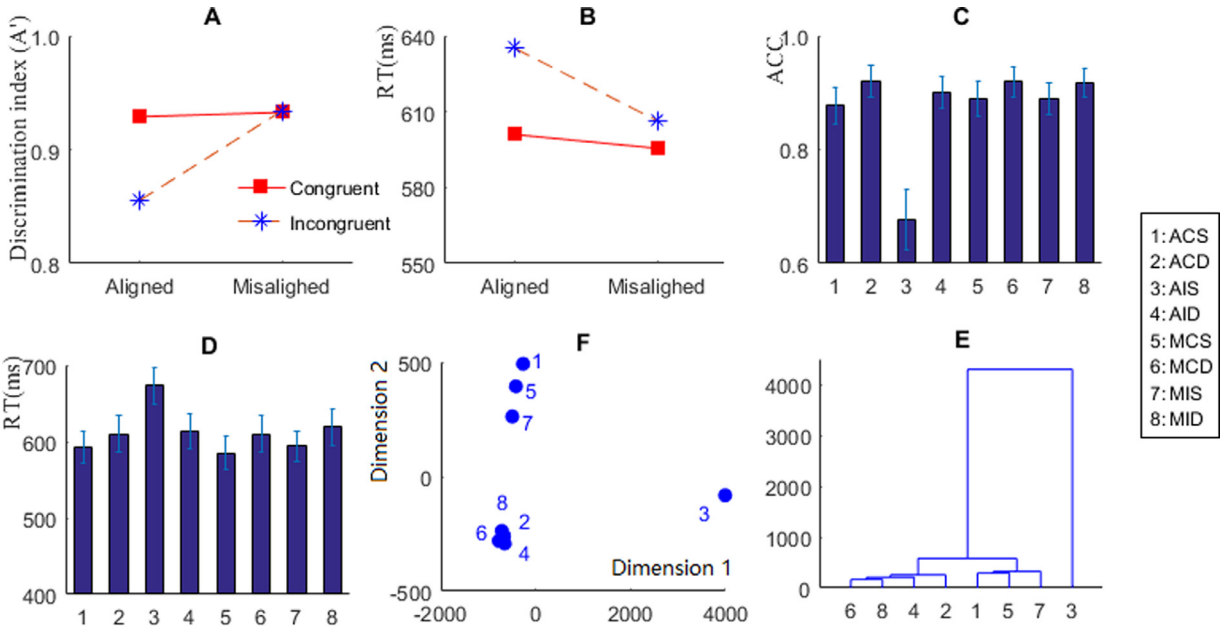

Fig. 2. The behavioral results in the complete composite paradigm (CCP). There is **(A)** significant main effect of congruency, main effect of alignment and the interaction between alignment and congruency in the discrimination index, **(B)** significant main effects of congruency and alignment in reaction time. **(C)** The accuracy and **(D)** reaction time of the 8 conditions in the CCP task. **(E)** The three major clusters among the 8 conditions revealed by hierarchical clustering analysis, and **(F)** the distribution of these clusters along the two major dimensions from multidimensional scaling analysis. (legend labels denote the 8 conditions, ACS: aligned congruent same, ACD: aligned congruent different, AIS: aligned incongruent same, AID: aligned incongruent different, MCS: misaligned congruent same, MCD: misaligned congruent different, MIS: misaligned incongruent same, MID: misaligned incongruent different).

where elements in the neural dissimilarity matrix were randomized and correlated to the behavioral matrix in each permutation. The correspondence was significant if the output index was among the lowest 50 in the permutation results (equal to $q \leq 0.05$ by Bonferroni correction).

2.7. Whole-brain searchlight analysis

To explore regions outside the above-identified ROIs that also demonstrated significant behavioral-neural correspondence, we conducted whole-brain searchlight analyses with the afore-mentioned multidimensional scaling and Spearman's-rank correlation. Specifically, the beta values of the 8 conditions were estimated by GLM analysis based on normalized but spatially unsmoothed images and extracted from a searchlight with radius of 3 voxels (Anzellotti et al., 2014). The voxels by conditions matrix within the searchlight was then centralized to compute the dissimilarity matrix based on the Euclidean distance, which was then correlated with the reference behavioral dissimilarity matrix by Spearman's Rank correlation. The correlation parameters images were then spatially smoothed with a kernel of FWHM of 6 mm. Significant clusters were determined based on Monte-Carlo simulation with the 3dClustSim function in AFNI, where the spherical autocorrelation –acf function parameters were determined by 3dFWHMx.

2.8. Data and code availability statement

Behavioral data, scripts for data analysis is available via https://osf.io/fsqaj/, fMRI Data can be accessed from the first author on request upon a formal data usage agreement.

3. Results

3.1. Behavioral results

We first analyzed the effect of alignment and congruency on discrimination sensitivity following the conventional procedure. Discrimination index was estimated individually for each of the alignments by congruency combinations by the following formula: (Stanislaw and Todorov, 1999): $A' = 0.5 + sign(H - F)\frac{(H-F)^2+|H-F|}{4max(H,F)-4HF}$, where H indicated hit rate and F indicated false alarm rate. Two-way ANOVA analysis (see Fig. 2A) revealed a significant main effect of alignment ($F(1,21) = 23.794$, $p < 0.001$, $\eta_p^2 = 0.531$) and congruency ($F(1,21) = 22.317$, $p < 0.001$, $\eta_p^2 = 0.515$), the discrimination sensitivity was generally higher in the misaligned trials than aligned trials, and higher in congruent trials than incongruent trials. There was also a significant alignment by congruency interaction ($F(1,21) = 28.142$, $p < 0.001$, $\eta_p^2 = 0.573$). Further analysis showed that the discrimination index was significantly lower in the incongruent condition than in the congruent condition when faces were aligned ($F(1,21) = 26.833$, $p < 0.001$, $\eta_p^2 = 0.561$), but with no congruency effect when faces were misaligned ($F(1,21) = 0.165$, $p = 0.689$, $\eta_p^2 = 0.008$). As for reaction time (see Fig. 2B), there was a significant main effect of alignment ($F(1,21) = 46.992$, $p < 0.001$, $\eta_p^2 = 0.691$), main effect of congruency ($F(1,21) = 85.635$, $p < 0.001$, $\eta_p^2 = 0.803$), and significant alignment by congruency interaction ($F(1,21) = 25.189$, $p < 0.001$, $\eta_p^2 = 0.545$). The reaction time was generally slower in the aligned than the misaligned condition, and slower in the incongruent trials than congruent trials. It was slower in the "incongruent" than the "congruent" condition both when the face parts were aligned ($p < 0.001$) and misaligned ($p < 0.001$), the interaction however, suggested the congruency effect in misaligned trials was smaller than that in the aligned trials.

To characterize in-detail the response pattern, we conducted a repeated-measures ANOVA on accuracy and reaction time of all 8 conditions. The analysis revealed a significant three-way interaction in accuracy ($F(1,21) = 25.292$, $p < 0.001$, $\eta_p^2 = 0.546$, Figure 2C) and reaction time ($F(1,21) = 59.462$, $p < 0.001$, $\eta_p^2 = 0.739$, Fig. 2D). A simple effect analysis on accuracy found a congruency by response interaction when faces were aligned ($F(1,21) = 18.191$, $p < 0.001$, $\eta_p^2 = 0.464$) but not misaligned ($F(1,21) = 2.522$, $p = 0.127$). When faces were aligned, response accuracy in congruent trials was higher than the incongruent trials regardless of the response type ("same", $F(1,21) = 23.412$, $p <$

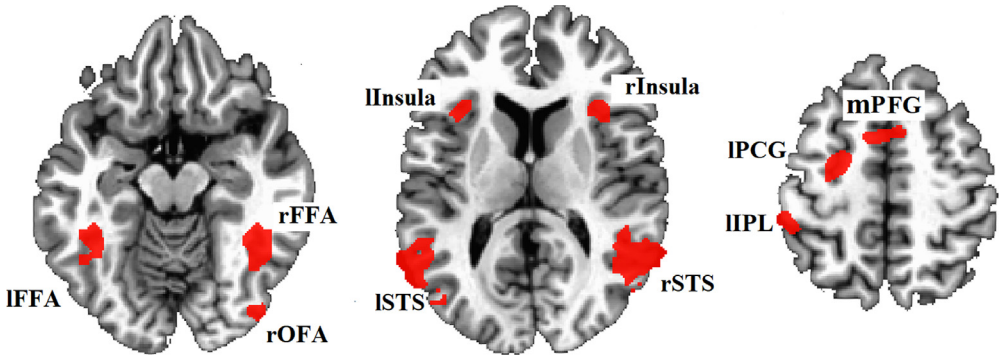

Fig. 3. The ROIs identified by idenpendent localizer scanning. The face recognition task revealed 5 regions of the face network: the right Fusiform Face Area (rFFA), the left Fusiform Face Area (lFFA), the right Superior Temporal Sulcus (rSTS), the left Superior Temporal Sulcus (lSTS) and the right Occipital Face Area (rOFA). The eriksen flanker task identified 5 ROIs within the attention network: right anterior insula, left anterior insula, dorsal medial prefrontal cortex (mPFC), left inferior parietal lobe (lIPL) and left precentral gyrus (lPCG).

0.001, $\eta_p^2 = 0.527$, "different", $F(1,21) = 5.29$, $p = 0.032$, $\eta_p^2 = 0.201$), but the significant interaction indicated a higher congruency effect in aligned over misaligned faces. As for the three-way interaction in RT, there was an interaction between congruency and response when faces were aligned ($F(1,21) = 87.672$, $p < 0.001$, $\eta_p^2 = 0.807$), but not when they were misaligned ($F(1,21) = 0.878$, $p = 0.359$). In the aligned trials, RT in the incongruent condition was longer than that in the congruent condition when the correct response was "the same" ($F(1,21) = 111.908$, $p < 0.001$, $\eta_p^2 = 0.842$), but there was no congruency effect when the correct response was "different" ($F(1,21) = 1.098$, $p = 0.307$). In both accuracy and reaction time, there was also a main effect of alignment (ACC: $F(1,21) = 23.193$, $p < 0.001$, $\eta_p^2 = 0.525$, RT: $F(1,21) = 53.245$, $p < 0.001$, $\eta_p^2 = 0.717$), as well as alignment by congruency interaction (ACC, $F(1,21) = 36.184$, $p < 0.001$, $\eta_p^2 = 0.633$, RT: $F(1,21) = 42.916$, $p < 0.001$, $\eta_p^2 = 0.671$), alignment by response interaction (ACC: $F(1,21) = 21.546$, $p < 0.001$, $\eta_p^2 = 0.506$, RT: $F(1,21) = 34.735$, $p < 0.001$, $\eta_p^2 = 0.623$), and congruency by response interaction (ACC, $F(1,21) = 11.851$, $p < 0.001$, $\eta_p^2 = 0.361$, RT: $F(1,21) = 45.359$, $p < 0.001$, $\eta_p^2 = 0.684$).

Next, we employed hierarchical clustering and multidimensional scaling analysis to explore the structure among the 8 conditions. These dimension reduction techniques enable us to explore relationships among conditions via a data-driven approach. Dissimilarity matrices for these two analyses were built based on the inverse efficiency score (RT/ACC) in each condition, which has the advantage of combining the effect of both indices (Bruyer and Brysbaert, 2011; Townsend and Ashby, 1978). We also estimated the percentage of variance explained by each component based on the eigenvalues available in multidimensional scaling analysis. The results showed that the first dimension accounted for 95.18% and the second dimension accounted for 3.93% of the total variance in the inverse efficiency score. It is worth noting that similar results were also obtained in analysis on accuracy, with 85.50%, 10.53% of the variance explained by the first and second components respectively (see supplementary materials).

As shown in Fig. 2E, we identified three clusters from behavioral response of the 8 conditions. The first cluster contained only the AIS condition (alignment: aligned, congruency: incongruent, response: same), which was distant from all other conditions. The second included the ACD (aligned, congruent, different), AID (aligned, incongruent, different), MCD (misaligned, congruent, different), and MID (misaligned, incongruent, different) conditions, where the target halves were all "different". The third cluster contained the MCS (misaligned, congruent, same), MIS (misaligned, incongruent, same) and ACS (aligned, congruent, same) conditions where the target halves were all "the same". We could see in Fig. 2F the first dimension generated by multidimensional scaling analysis was largely characterized by how far away the AIS condition was from all other 7 conditions, while the second dimension reflected largely the type of response, with all conditions of the response "different" at one end and most conditions of the response "same" at the other end. Similar dimensions and clusters were replicated in analyses on accuracy (see supplementary materials).

3.2. FMRI results in localizer scanning

Face processing network: Five major regions, including the right Fusiform Face Area (rFFA), the left Fusiform Face Area (lFFA), the right Superior Temporal Sulcus (rSTS), the left Superior Temporal Sulcus (lSTS) and the right Occipital Face Area (rOFA) were identified individually for the participants (see Fig. 3). The average coordinates, number of voxels, and ratio of positive participants are available in Table 1, detailed information including the coordinates, number of voxels, threshold of each participant can be seen in the supplementary materials (see also in Tables S2–8).

Attentional Network: Group analysis revealed 5 major clusters after FDR correction (Table 2, Fig. 3), which included the right anterior insula, left anterior insula, dorsal medial prefrontal cortex (mPFC), left inferior parietal lobe (lIPL) and left precentral gyrus (lPCG). These regions replicated the classical results found in previous studies (Casey et al., 2000).

3.3. Univariate analysis in the composite face task

Next, we ran a 2 by 2 by 2 ANOVA analysis to explore the impact of the three factors (alignment, congruency, response type) on BOLD response in each ROI (Fig. 4, Figures S5-1-10). In regions of the face network, there were significant main effects of alignment in left FFA ($F(1,21) = 15.217$, $p = 0.001$, $\eta_p^2 = 0.420$), right STS ($F(1,21) = 12.224$, $p = 0.002$, $\eta_p^2 = 0.368$), both survived Bonferroni-correction for N = 10 ROIs. There was main effect of alignment in right FFA ($F(1,20) = 9.553$, $p = 0.006$, $\eta_p^2 = 0.323$), right OFA ($F(1,19) = 5.500$, $p = 0.030$, $\eta_p^2 = 0.224$) which did not survive the Bonferroni-correction (N = 10 ROIs). In the first four regions, the BOLD response was generally higher in the aligned trials than the misaligned trials. There was also a main effect of response type in the right OFA ($F(1,19) = 10.877$, $p = 0.004$, $\eta_p^2 = 0.364$), with higher beta value in trials with the response "different" than those with the response "the same". No other effects were observed within the face network, $p > 0.100$.

As for regions in the attention network, there were main effects of alignment in the left anterior insula ($F(1,21) = 11.671$, $p = 0.003$, $\eta_p^2 = 0.357$, surviving Bonferroni-correction for N = 10 ROIs), right anterior insula ($F(1,21) = 7.884$, $p = 0.011$, $\eta_p^2 = 0.273$) and mPFG ($F(1,21) = 5.086$, $p = 0.035$, $\eta_p^2 = 0.195$) which did not survive Bonferroni-correction, with higher response in the aligned trials over the misaligned trials. There were also main effects of congruency in the right anterior insula ($F(1,21) = 18.622$, $p < 0.001$, $\eta_p^2 = 0.470$), mPFG ($F(1,21) = 17.593$, $p < 0.001$, $\eta_p^2 = 0.456$). In all three areas, BOLD response in the incongruent trials was higher than that in the congruent trials. There were main effects of response type in the right anterior in-

Table 1
The characteristics of face processing areas.

ROI	*X*	*Y*	*Z*	voxels	ratio
rFFA	40.5 ± 3.55	-45.929 ± 5.418	-15.5 ± 3.674	60.222 ± 41.347	21/22
lFFA	-39.545 ± 4.572	-47.591 ± 8.047	-15.909 ± 7.249	40.182 ± 29.936	22/22
lSTS	-47.318 ± 8.342	-57.545 ± 11.086	8.773 ± 7.685	90.455 ± 72.072	22/22
rOFA	37.95 ± 6.329	-74.85 ± 7.631	-11.15 ± 5.284	46.9 ± 61.068	20/22
rSTS	52.364 ± 7.882	-52.091 ± 10.404	6.591 ± 6.248	126.857 ± 89.337	22/22

Table 2
The characteristics of the attentional network.

ROI	*X*	*Y*	*Z*	voxels
rInsula	34.5	16.5	14.5	54
lInsula	-31.5	16.5	14.5	39
lPCG	-25.5	-7.5	53.5	117
lIPL	-46.5	-37.5	44.5	134
mPFG	-10.5	4.5	50.5	55

sula ($F(1,21) = 13.328$, $p = 0.001$, $\eta_p^2 = 0.388$), and left anterior insula ($F(1,21) = 12.343$, $p = 0.002$, $\eta_p^2 = 0.370$) where neural activity in the "same" trials was higher than that in the "different" trials. There were also alignment by congruency interactions in the right anterior insula ($F(1,21) = 8.410$, $p = 0.009$, $\eta_p^2 = 0.286$) and mPFG ($F(1,21) = 4.312$, $p = 0.05$, $\eta_p^2 = 0.170$) which did not survive Bonferroni-correction. In both areas, the incongruent trials elicited relatively higher response than the congruent trials (right anterior insula, $p < 0.001$, mPFG, $p = 0.001$) when face halves were aligned, but not when faces were misaligned (right anterior insula, $p = 0.409$, mPFG, $p = 0.301$). We also observed interactions between alignment and response type in right anterior insula ($F(1,21) = 9.137$, $p = 0.006$, $\eta_p^2 = 0.303$), left anterior insula ($F(1,21) = 6.026$, $p = 0.023$, $\eta_p^2 = 0.223$), and mPFG ($F(1,21) = 5.025$, $p = 0.036$, $\eta_p^2 = 0.193$) which did not survive Bonferroni-correction. In all three areas, trials with the response "same" induced higher response than those with the response "different" when face halves were aligned (right anterior insula, $p < 0.001$, mPFG, $p < 0.001$, the left anterior insula, $p < 0.001$), but not when face halves were misaligned (right anterior insula, $p = 0.077$, mPFG, $p = 0.67$, left anterior insula, $p = 0.147$). The response type also interacted with congruency in right anterior insula ($F(1,21) = 4.666$, $p = 0.042$, $\eta_p^2 = 0.182$). Trials with the response "same" induced higher response than the trials with the response "different" in the incongruent condition ($p < 0.001$), but did not differ from each other in the congruent condition ($p = 0.370$). There was no response by congruency interaction in left anterior insula ($F(1,21) = 3.473$, $p = 0.076$), nor mPFG ($F(1,21) = 0.504$, $p = 0.485$). As for the other two regions identified by Eriksen Flanker task, namely the left inferior parietal lobule and left precentral gyrus, there was no main effect of alignment, congruency, or response, nor interaction between any two factors or three factors ($p > 0.05$ uncorrected).

Importantly, there were three-way interactions in right anterior insula ($F(1,21) = 7.239$, $p = 0.014$, $\eta_p^2 = 0.256$) and mPFG ($F(1,21) = 5.042$, $p = 0.036$, $\eta_p^2 = 0.194$), though both failed surviving the Bonferroni correction for 10 ROIs. Simple effect analysis showed that in these areas, there was a significant interaction between congruency and response type in aligned faces (right anterior insula, $F(1,21) = 9.058$, $p = 0.007$, $\eta_p^2 = 0.301$, mPFG ($F(1,21) = 4.121$, $p = 0.055$, $\eta_p^2 = 0.164$), but not in misaligned faces (right anterior insula, $F(1,21) = 0.184$, $p = 0.672$, mPFG, $F(1,21) = 0.909$, $p = 0.351$). The interaction in aligned faces was characterized by higher BOLD response in incongruent condition over the congruent condition when the top halves were "the same" (right anterior insula ($F(1,21) = 25.93$, $p < 0.001$, $\eta_p^2 = 0.552$), and mPFG ($F(1,21) = 18.487$, $p < 0.001$, $\eta_p^2 = 0.468$), but no congruency effect when the top halves were "different" (right anterior insula, $F(1,21) = 0.249$, $p = 0.623$, mPFG, $F(1,21) = 0.557$, $p = 0.464$).

3.4. Behavioral-neural correspondence in ROIs

The results of multidimensional scaling analysis and hierarchical clustering on BOLD signal in the ten ROIs are available in Fig. 5. Hierarchical clustering revealed three consistent clusters among the 8 con-

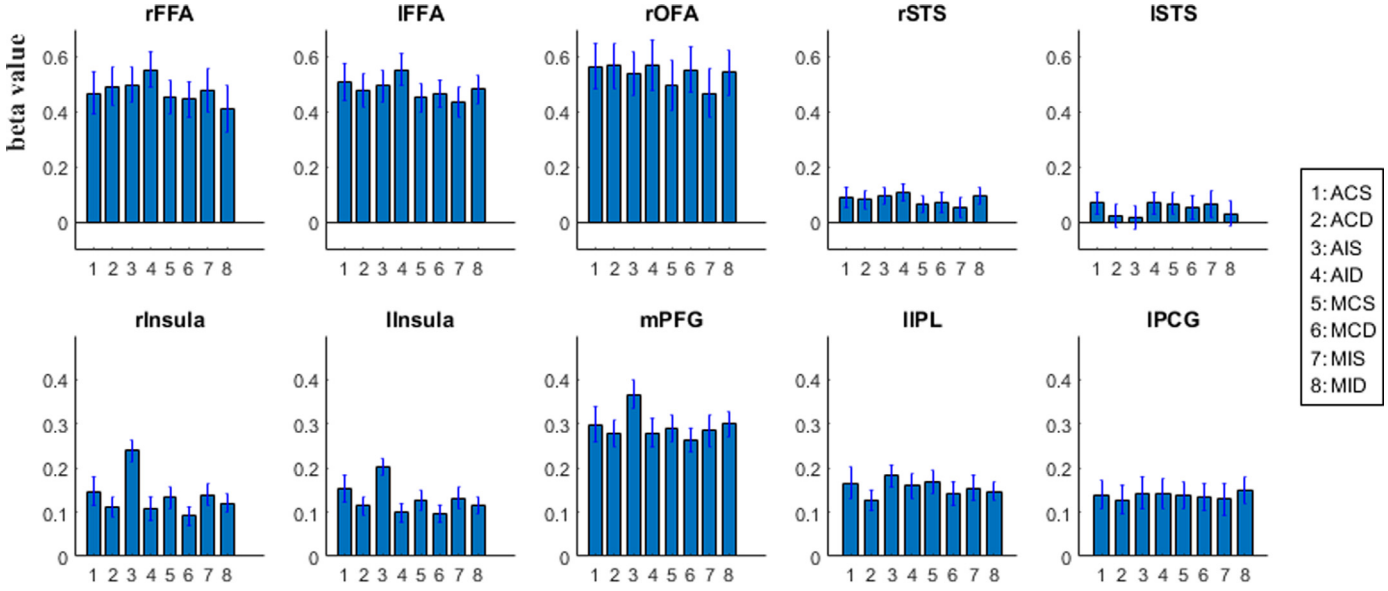

Fig. 4. Beta values of the conditions in each ROI.

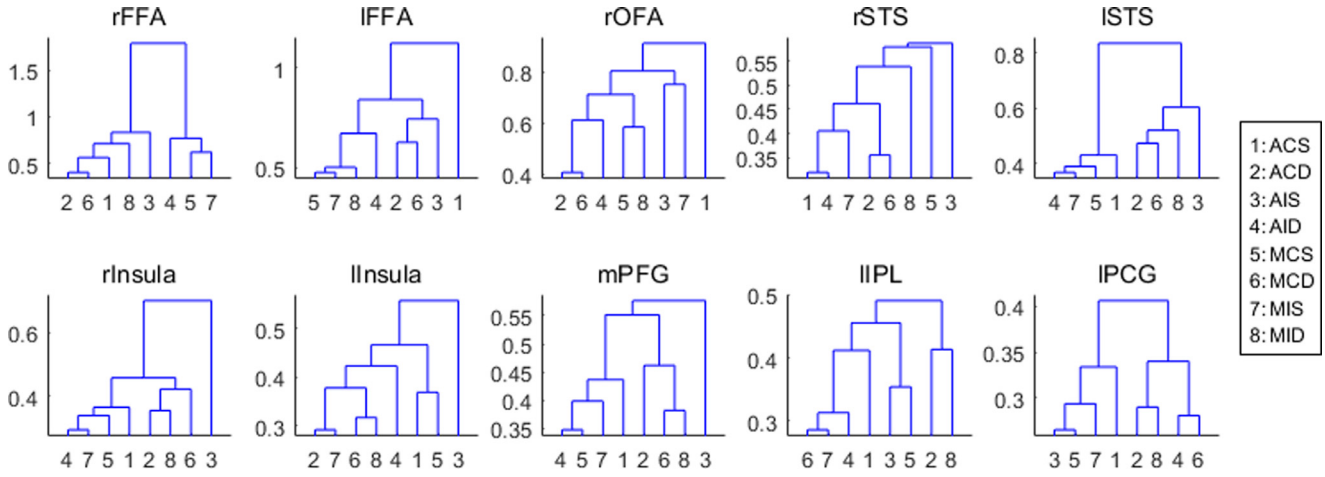

Fig. 5. The clustering revealed by dendrograms among the experimental conditions in each ROI. The right insula, left insula and medial prefrontal gyrus demonstrate similar proximity structure among the 8 experimental conditions as in the behavioral response.

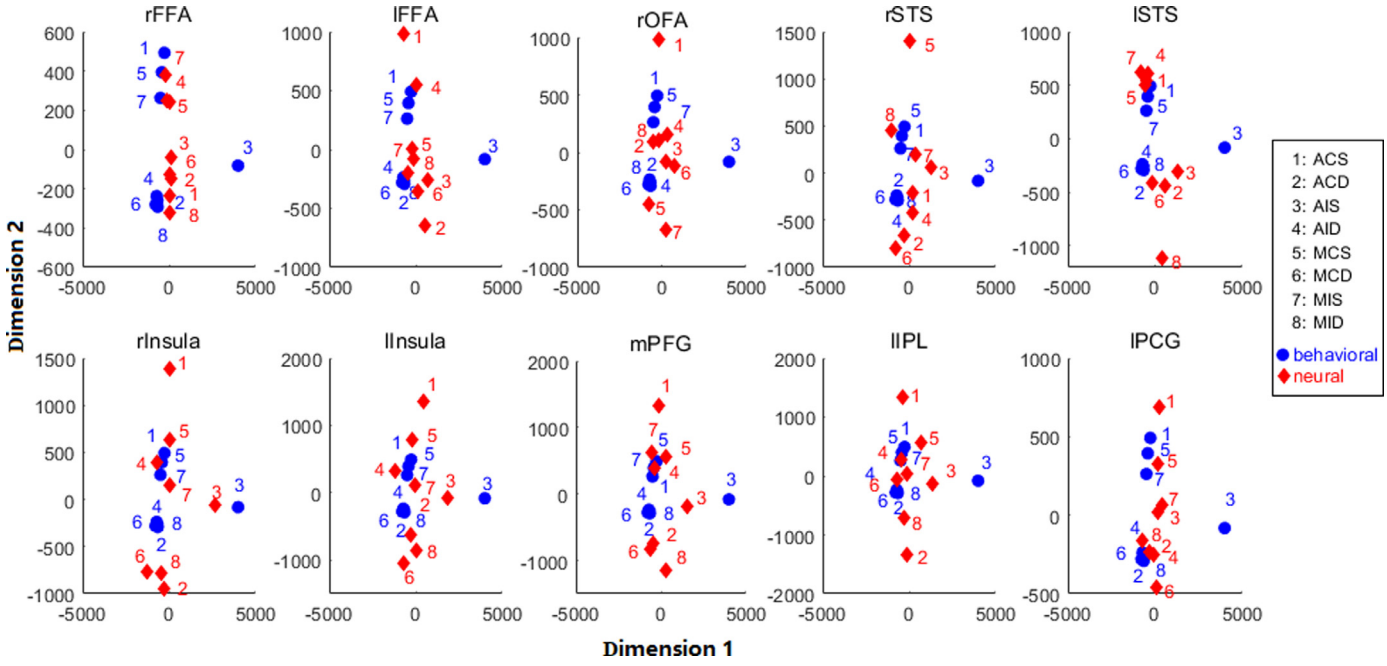

Fig. 6. Distribution of the 8 conditions along the two principal dimensions by the multidimensional scaling analysis. blue dots: conditions in behavioral data, red dots: conditions in neural data.

ditions in areas including the bilateral insula and the mPFG. In all three areas, the first cluster included only one condition: (AIS), which was distant from all the other conditions. The second cluster consisted of the ACD, MCD and MID conditions, where the correct response was all "different". The third condition contained the ACS, AID, MCS and MIS conditions, where the correct response was mostly "the same" except the AID condition. The patterns of clustering in the other areas did not convey explicit information either about response type or attentional control. Multidimensional scaling analysis on dissimilarity matrix extracted two major dimensions among neural response of these 8 conditions in bilateral insula and the mPFG. As can be seen in Fig. 6, the first dimension generated by the multidimensional scaling analysis was largely characterized by the distance of the AIS condition away from all other 7 conditions. The second dimension reflected mainly the type of response, with most of the conditions with the response "different" at one end and most conditions with the response "same" at the other end.

To explore brain regions where the neural activities fit satisfactorily to the behavioral results, we estimated the behavioral and neural dissimilarity matrices of the 8 conditions, and matched them by the Spearman's rank correlation. Permutation simulation analysis (n = 10,000) on the correlation, as plotted in Fig. 6, showed significant neural-behavioral correspondence in the right anterior insula ($p < 0.001$), left anterior insula ($p < 0.001$), both survived the Bonferroni multiple correction for $N = 10$ ROIs. The neural pattern in mPFG also matched that of the behavioral results ($p = 0.006$), with a significance trending to $q < 0.05$ by Bonferroni correction. In contrast, the neural-behavioral conformation was not significant in any of the 5 face processing regions (for right OFA, $p = 0.113$, right STS, $p = 0.319$, left FFA, $p = 0.391$, left STS, $p = 0.329$, right FFA, $p = 0.856$). These results suggested the neural response in the bilateral insula areas showed better fitting to the pattern in the behavioral data than areas in the face processing network. It is also worth noting that similar results were obtained when the reference behavioral dissimilarity was estimated based on response accuracy (see supplementary information).

To assess the reliability of clustering across participants, we used a n-fold cross-validation technique (Chen et al., 2015; Qin et al., 2014)

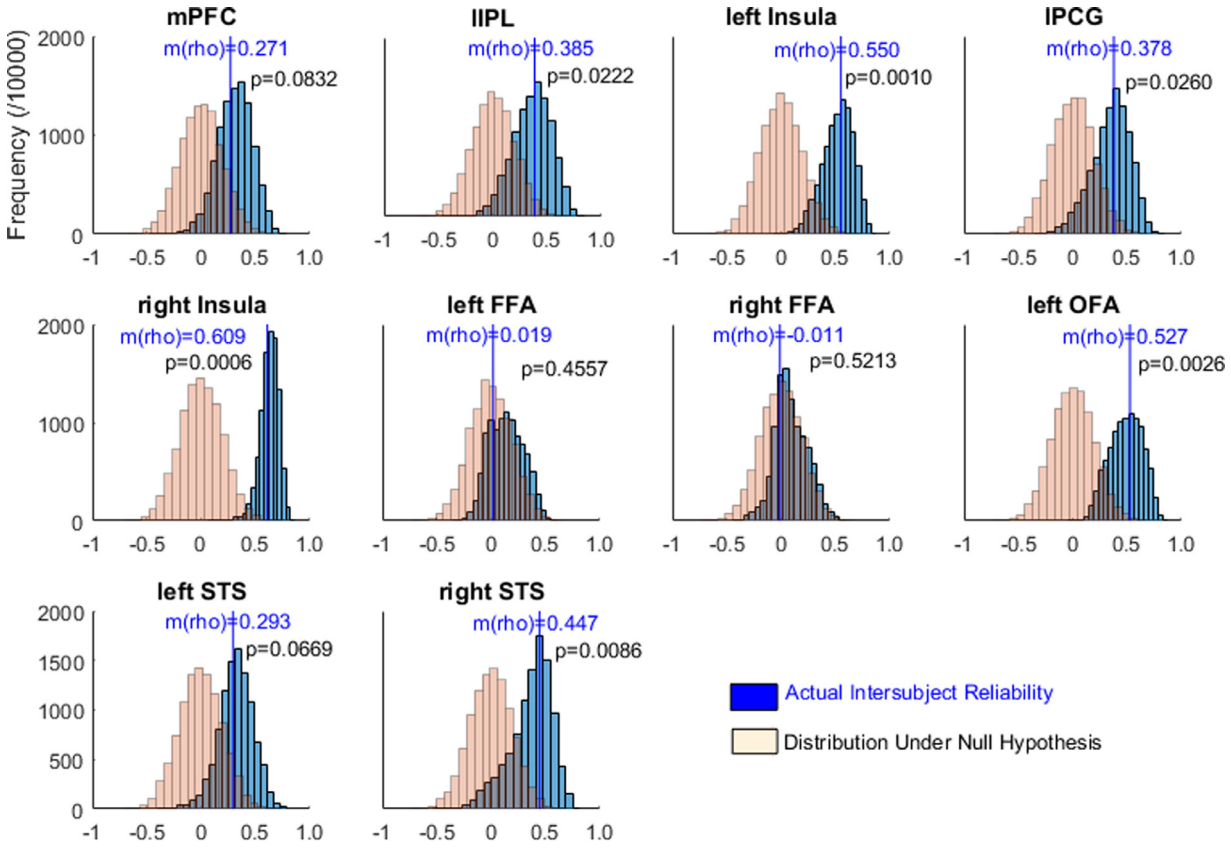

Fig. 7. Inter-subject reliability in clustering tested by the N-fold cross-validation. Regions including right insula, left Insula, left OFA showed consistency across participants in the clustering. ($P < 0.005$, corrected for multiple comparison of $N = 10$ ROIs).

based on the dissimilarity indices as recommended in previous studies (Walther et al., 2016). The Euclidean distances among the 8 experimental conditions, based on of beta values in unsmoothed first-level GLM statistical maps, were divided into a learning set and a test set. We used a four-fold strategy (Qin et al., 2014; Varoquaux, 2018) that 3/4 of the participants were assigned to the learning set and the remaining 1/4 to the test set via a random permutation procedure. The averaged Euclidean distances ($n = 28$) in the learning set were then correlated with those in the test set based on the Spearman Rank (Levine and Schwarzbach, 2021; Popal et al., 2020). This procedure was iterated for 10,000 times to generate a distribution of correlation coefficients from the observed data ($R_{observed}$). The same procedure was used to obtain the distribution under the null hypothesis that there was no consistency among participants, where the correlation was carried out after randomizing elements of the Euclidean distances (R_{null}). The inter-participant stability was indexed by percentage of cases in R_{null} higher than the mode of $R_{observed}$, and the significance was determined at $p < 0.005$ corrected for multiple comparisons of $n = 10$ ROIs. As shown in Fig. 7, there was significant inter-subject stability in the region of the right insula ($p = 0.0006$), left insula ($p = 0.001$), left OFA ($p = 0.0026$), which survived the correction for multiple comparisons. Other regions, including medial prefrontal cortex ($p = 0.083$), left inferior parietal lobule ($p = 0.022$), left precentral gyrus ($p = 0.026$), left FFA ($p = 0.456$), right FFA ($p = 0.521$), left STS ($p = 0.067$), right STS ($p = 0.008$) did not show satisfactory inter-subject stability. Clustering i of each participant is available in Figs. S6-2 to S6-11.

3.5. Whole-brain searchlight based on behavioral-neural correspondence

To explore cortical regions with significant behavioral-neural correspondence outside the ROIs identified by the localizer scanning, we conducted searchlight analysis across the whole-brain gray matter areas based on Spearman's rank correlation between response dissimilarity matrices. This revealed significant neural-behavioral conformation in additional areas encompassing frontal cortices including bilateral superior frontal gyrus (SFG), middle frontal gyrus (MFG), and the right inferior frontal gyrus (rIFG), the anterior cingulate cortex (ACC), posterior cingulate cortex (PCC), the cuneus and precuneus, and right inferior temporal gyrus (rITG, Fig. 8). The significance was decided using a stringent height-threshold of $p < 0.0001$ and extent threshold of at least 42 continuous voxels, based on Monte-Carlo simulation with the 3dClustSim function in AFNI (for the acf parameter in 3dClustSim: $a = 0.343981$, $b = 7.37927$, $c = 23.8731$, with alpha=0.01). When the Euclidean distances in the primary visual cortex were used as a covariate, multiple regression analyses revealed significant association between the behavioral dissimilarity pattern and the neural dissimilarity in right insula, $t(25) = 3.482$, $p = 0.002$; left insula, $t(25) = 3.293$, $p = 0.003$; PCC, $t(25) = 2.952$, $p = 0.007$, medial prefrontal gyrus, $t(25) = -2.125$, $p = 0.044$; and inferior temporal gyrus, $t(25) = 5.377$, $p < 0.001$, left middle PFG, $t(25) = 2.458$, $p = 0.021$; right middle PFG, $t(25) = 3.197$, $p = 0.004$; right inferior PFG, $t(25) = 5.642$, $p < 0.001$, which suggested robustness of predictability of these regions even after controlling for low-level information. The regression was not significant in ACC, $t(25) = 0.038$, $p = 0.970$; medial PFG, $t(25) = -0.347$, $p = 0.732$; left SFG, $t(25) = -0.543$, $p = 0.592$; right SFG, $t(25) = -1.692$, $p = 0.103$.

3.6. Whole-brain searchlight on the neural RSA relevance of the alignment effect

Since the alignment effect is one of the frequently cited features of holistic face processing (Foster et al., 2021; Rossion, 2013; Young et al., 1987), we then explored the cortex where the neural representational

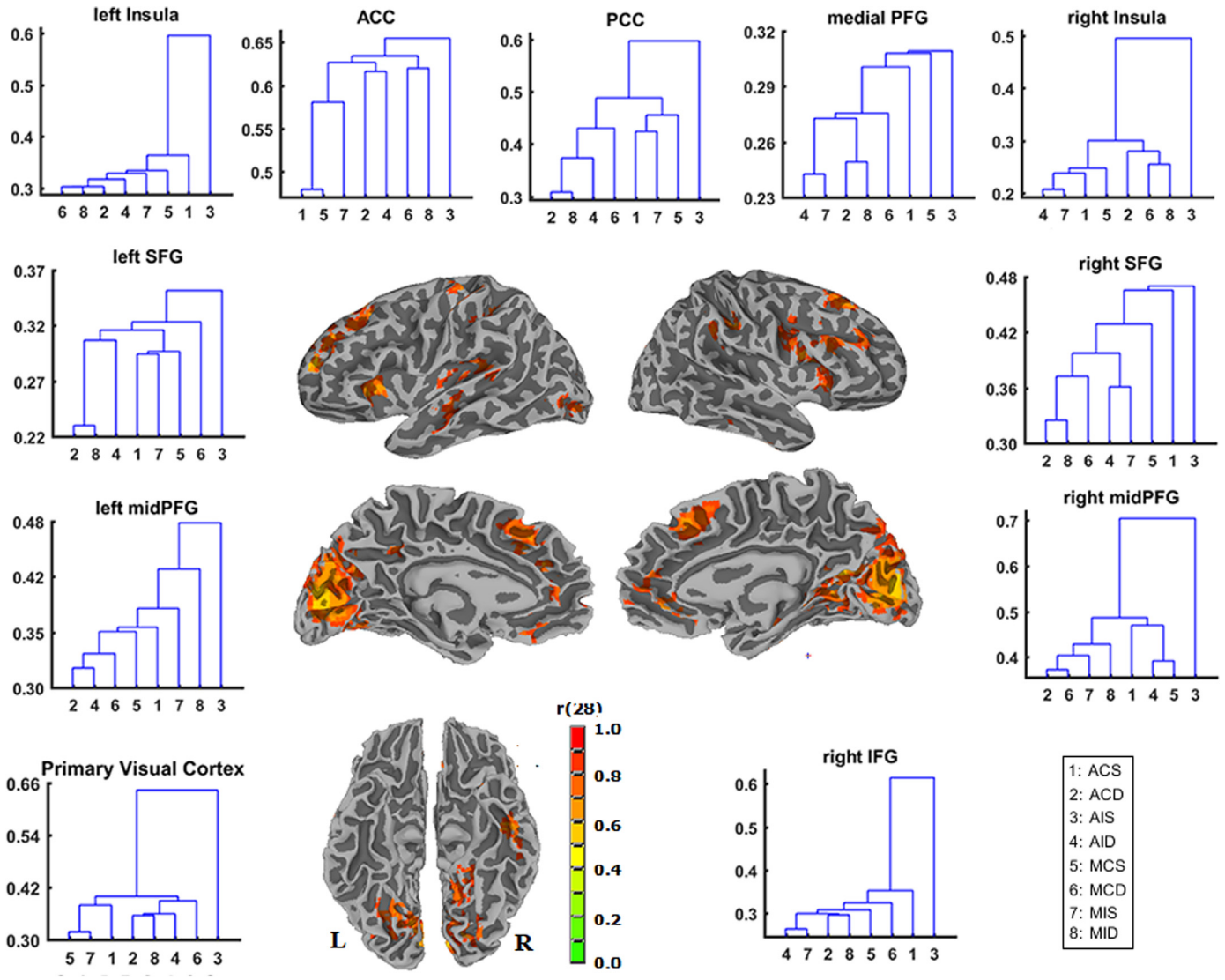

Fig. 8. Searchlight analysis based on the dissimilarity among all 8 conditions. This reveals significant behavioral-neural conformation in the bilateral prefrontal cortex, the cuneus and precuneus, and the right inferior temporal gyrus along with bilateral insula.

similarity was organized along the aligned versus misaligned conditions via a whole-brain searchlight analysis with model driven representational dissimilarity matrix (RDM). We constructed a candidate RDM (see in Fig. 9A) that assumed separate clusters within the aligned and misaligned conditions (intra-cluster dissimilarity indices of 0, and inter-cluster indices of 1; Kriegeskorte et al., 2008). The candidate RDM was then correlated with the neural dissimilarity based on the Spearman Rank, through a whole-brain searchlight procedure. The searchlight analysis revealed two significant clusters in the occipital cortex, at the height threshold of $p < 0.001$ and the extent threshold of 70 voxels, with alpha=0.05 by 3dClustSim function in AFNI. The dendrograms among the conditions are shown in (Fig. 9B): in both regions all the aligned conditions cluster together and all the misaligned conditions formed another cluster.

4. Discussion

In this study, we investigated the neurocognitive relevance of the characteristic behavioral CFE effect using the complete composite paradigm (CCP task). There were two features worth-noting. First, going beyond previous research that focused primarily on the perceptual network (Foster et al., 2021; Schiltz et al., 2010; Schiltz and Rossion, 2006), we explored the contribution of the face network and attention network via independent localizer scanning. Second, complementing conventional results based on univariate contrasts, we used dimension reduction techniques to reveal the relationship among all the experimental conditions in the CCP measurement, and identified the major contributors to the observed behavioral performance. We conducted ROI-based and whole-brain searchlight analysis based on behavioral-neural correspondence to explore the cortical hubs whose neural response best fit the pattern of behavioral responses. The results form a bridge between attention and holistic face processing, and provided a more comprehensive picture about the neurocognitive operations underlying the composite face effect.

4.1. Contribution of attentional inference and response decision as revealed by model-free analyses on behavioral data

The clusters and dimensions revealed by our data-driven analysis provide a new line of evidence for the coexistence of attentional (Boutet et al., 2002; Fitousi, 2015, 2016) and decisional components (Fitousi, 2020; Richler et al., 2008) in the composite face effect. We identified three distinct clusters among the 8 experimental conditions in the behavioral data via hierarchical clustering analysis and extracted

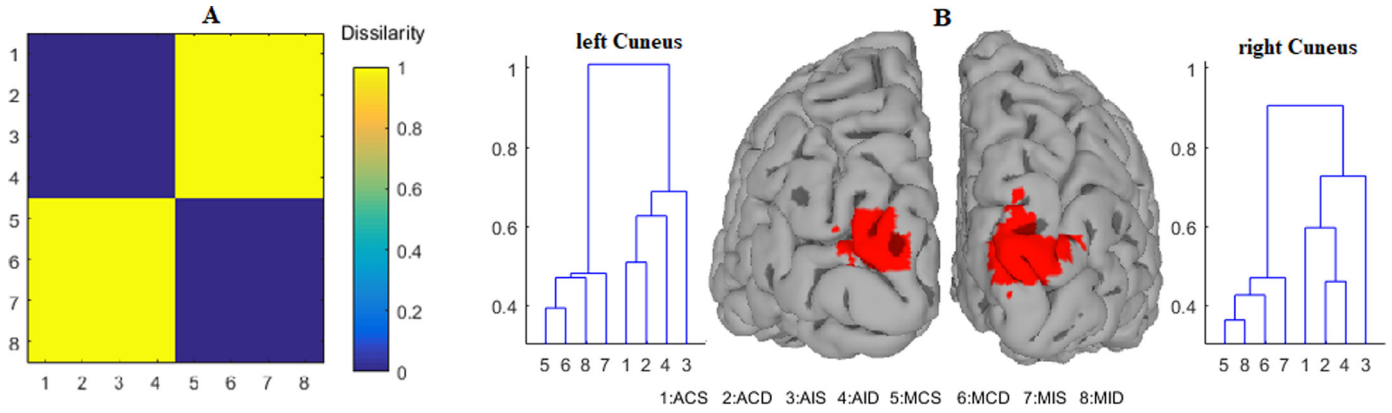

Fig. 9. Searchlight results on alignment effect. (A) the candidate representational dissimilarity matrix, (B) two clusters in the cuneus were found with neural similarity organized along the aligned versus misaligned dimension.

two principal dimensions by classical multidimensional scaling analysis. The first cluster consisted of the AIS condition only, the second cluster all the remaining conditions with correct response "same", while the third cluster all conditions with correct response "different". Importantly, the distribution profile of the three clusters revealed by the multidimensional scaling analysis suggest the contributing factors to the behavioral data. Since the first dimension is characterized mainly by the distance between AIS (the first cluster) and all other conditions (the latter two clusters), it probably reflects attentional interference or cognitive control because in the composite face task because the AIS results into significantly more failure in selective attention over all the other conditions. The first dimension cannot be explained by perceptual operations, because the AIS condition is distinguishably distant from ACS, AID and ACD despite the faces in all the four conditions are spatially aligned. The second dimension is probably driven by response decision in the CCP paradigm as it is characterized mainly by the proximity between the conditions requiring "same" response and those requiring "different" response.

The contribution of these two cognitive loci could be ideally supported by existent findings from computational modelling. Employing a multidimensional generalization of signal detection theory that can distinguish between perceptual and decisional loci of holistic effects (Ashby and Townsend, 1986; Richler et al., 2008, 2009) observed consistent violations of perceptual separability and decisional separability but little violation of perceptual independence. This was observed both in the composite face tasks requiring divided attention and those requiring selective attention. The perceptual and decisional separability were also observed in a later set of behavioral and ERP studies (Von Der Heide et al., 2018). Consistent with a mechanism rooted in category-specific learned attention, it was further found that learned attention to parts or components was sufficient to result in holistic processing (Gauthier, 2020). Analyses on the theoretical ex-Gaussian parameters of RT distributions (Fitousi, 2020) also indicate that the CFE effect is generated by pure changes in the exponential component of the ex-Gaussian distribution, which suggests the involvement of attentional and working memory processes in the composite face effect regardless of partial and complete designs.

4.2. *The behavioral-neural correspondence in attention network*

The involvement of attentional and cognitive control is further supported by the significant behavioral-neural correspondence observed in the anterior insula and medial prefrontal cortex (mPFC). Our data revealed two interesting lines of behavioral-neural correspondence in these two regions. First, the triple-interaction in BOLD signals mirrored that found in the behavioral inverse efficiency score and accuracy. In both modalities, the congruency effect was stronger in aligned over misaligned faces when the top halves were "the same" but there was no alignment by congruency interaction when the top halves were "different". Second, the proximity of neural signals of the 8 experimental conditions was similar to that found in the behavioral responses, as visualized by the hierarchical clustering and strengthened by the significantly high Spearman's rank correlation between the behavioral and the neural dissimilarity structures.

The involvement of insula and prefrontal cortex are consistent with findings that have frequently been reported in previous studies on holistic or configural face processing (Rotshtein et al., 2007). For instance, these are activated both at long and short intervals when participants temporally integrate facial parts (Lee et al., 2012), and there is significant correlation between the behavioral and neural sensitivity to second-order configural relations in inferior frontal gyrus, superior frontal gyrus, cingulate gyrus and insula (Rotshtein et al., 2007). Areas including bilateral dorsolateral prefrontal cortex show highest response to the MIS condition than other conditions (Schiltz et al., 2010). When making same-different face judgements, there is higher activation in areas including the fusiform gyrus, medial frontal gyrus, inferior frontal cortex in the right hemisphere when the faces differed in terms of relational rather than featural aspects (Maurer et al., 2007). Critically, TMS over the right inferior frontal gyrus selectively interferes with configural processing of faces (Renzi et al., 2013). In a study using the partial composite face paradigm, Paparello (2007) found an alignment effect in the right anterior insula and medial frontal gyrus. The insular and prefrontal sensitivity to holistic face processing was correlated with the CFE effect: the activation in right insula was higher to aligned over misaligned faces in children performing better in the composite face task, but for children scoring lower in the task there was higher activation for misaligned than aligned trials in the medial frontal gyrus and anterior cingulate (Paparello, 2007).

Potential candidates such as working memory or emotion, which also elicit activation in insula and prefrontal cortex during face processing, are insufficient to explain the behavioral-neural correspondence in our data. First, all the face stimuli in our study were emotionally neutral, and second, working memory load was comparable for all 8 conditions because their intervals between study and test images were identical. We argue instead that it is attentional and cognitive control that most likely account for the response dissimilarity in these two regions. The human insular cortex is a heterogeneous brain structure that plays an integrative role in guiding behavior. The insula, especially the anterior portion of the insula, is critical for identifying salient sensory, affective, and cognitive cues for goal-directed attention (Craig, 2009; Menon and Uddin, 2010), conscious awareness (Huang et al., 2021). It is connected structurally and functionally with areas including the anterior cingulate, frontal, orbitofrontal areas (Uddin et al., 2017), constituting an integral part of the well-known salience network (Menon and Uddin, 2010) for

detecting and filtering salient stimuli and initiating attentional control signals (Uddin et al., 2017). The anterior insula is also a key structure of the cingulo-opercular network (CON), a subnetwork of the cognitive control circuit for conflict monitoring and resolution (Fan, 2014; Wu et al., 2021, 2020). The anterior insula as a hub that integrates interactions with large-scale brain networks (Menon et al., 2020; Menon and Uddin, 2010), volleying external sensory information with internal emotional and bodily state signals to coordinate brain network dynamics and to initiate switches between the default mode network (underlying self-related and social cognitive processes) and central executive network (which implements the maintenance and manipulation of information and decision making). This makes the anterior insula critical in identifying the most relevant information among multiple competing internal and external stimuli. This region plays a general role in task-level control and focal attention capture (Nelson et al., 2010), and links to executive control of attention (Eckert et al., 2009; Nee et al., 2007). As for the medial frontal gyrus, it plays a role in activities like attentional control (Nagahama et al., 1999) and decision making (Talati and Hirsch, 2005). There has been emerging evidence that the neural response in insular and frontal cortex to face processing is susceptible to attentional manipulations. For instance, participants with generalized social anxiety disorder exhibited greater insular activation compared to controls when attending to emotional faces (Klumpp et al., 2013). The magnitude of anterior insular response to facial signals of disgust was substantially reduced with reduced attention (Anderson et al., 2003).

Turning to the complete composite face paradigm, when the participants receive the task, their mission is to compare the target parts or components. However, the information from the irrelevant location is automatically activated due to holistic face processing (Rossion, 2013). When competing information or response tendencies are elicited in such circumstances, there arises pre-response conflict (Tso et al., 2017) and decision uncertainty (Botvinick et al., 2001), which herald an increased likelihood of failure. To solve conflict or gather necessary information for uncertainty reduction, additional attentional and control processes are imperative (Ullsperger et al., 2010). The participants have to inhibit concomitantly the interference from either the distractor parts (Richler et al., 2009; Richler et al., 2012) or from the global gestalt (Rossion, 2013) in order to best focus on the targets. These cognitive demands dovetail the functions of the anterior insula and medial frontal cortex, which, as reviewed briefly below, are consistently activated in circumstances calling for adjustments, specifically pre-response conflict and decision uncertainty (Ullsperger et al., 2010). Moreover, the activation of the right anterior insular cortex (AIC) has been established to increase monotonically as a function of cognitive load, reaching its plateau early and showing a significant correlation to the capacity of cognitive control (Wu et al., 2019). This may explain why the AIS (aligned, incongruent, same) condition, which is accompanied by the strongest response conflict and uncertainty, elicits the highest activation in the insula and medial prefrontal cortex than over all other conditions.

4.3. Holistic processing in both the “core” and “extended” face processing networks

The alignment effect in regions like FFA, pSTS, precuneus suggests holistic face processing in not only the “core” but also the “extended” face processing networks. Classical theories about face processing propose a hierarchically-organized system extending bilaterally from the inferior occipital gyri to the ventral anterior temporal lobes, with facial representations becoming increasingly complex and abstracted from low-level perceptual features as they move forward along this network (Nasr and Tootell, 2012). The “core system” consists of the fusiform face area (FFA), the occipital face area (OFA) and the posterior temporal sulcus (pSTS), whereas the “extended system” includes areas such as amygdala, precuneus, insula, anterior temporal lobe (Avidan et al., 2014; Gobbini and Haxby, 2006). There has been a wealth of evidence for holistic processing in the “core” system. For instance, transcranial direct current stimulation (tDCS) (Yang et al., 2014) or lesion (Busigny et al., 2010; Ramon et al., 2010) over occipito-temporal cortex would result in impairment of holistic face perception. The FFA is believed to host both holistic (Goffaux et al., 2013; Schiltz et al., 2010) and part-based representations of faces (Harris and Aguirre, 2008; Liu et al., 2010) and is sensitive to changes in both external and internal facial features (Andrews et al., 2010; Axelrod and Yovel, 2010; Kamps et al., 2019). In particular, previous studies using composite faces have found an alignment effect (Foster et al., 2021) or release of adaptation (Harris and Aguirre, 2010) in the FFA, positive association between the behavioral composite-face effect (CFE) and face selectivity in the right FFA (Li et al., 2017). The superior temporal sulcus (STS) is one of the cerebral cortices processing changeable facial aspects, such as facial expression, gaze (Kamps et al., 2019). It shares rich connections with the FFA (Zhang et al., 2009). Previous studies have shown activation when temporally integrating face parts (Lee et al., 2012), as well as robust sensitivity to face inversion (Chen et al., 2007) in bilateral superior temporal sulcus. The resting-state connection between bilateral pSTS and the FFA is closely linked to the behavioral composite face effect (Li et al., 2017).

Regions in the extended system are found to process semantic information and personal knowledge of faces (Gobbini and Haxby, 2006). The precuneus region displays functional connectivity with adjacent visual cortical regions (Margulies et al., 2009), it responds stronger to the visually familiar faces and plays a role in the retrieval of information from long-term memory and imagery (Gobbini and Haxby, 2006). Although the precuneus is among the consistently activated areas in face recognition (Gobbini and Haxby, 2006; Nasr and Tootell, 2012), its role in holistic face processing remains sparsely known. The significant behavioral-neural conformation observed in our study provides new evidence of holistic face processing in this region. It echoes previous findings that the precuneus is sensitive to face inversion, another hallmark of holistic face processing (Chen et al., 2007).

Though both are involved in the composite face effect, it is interesting that we see differentiable profiles between the “core” and “extended” face processing systems. The involvement of rFFA, STS is characterized primarily by a significant main effect of alignment, whereas the precuneus and insula demonstrate both a main effect of alignment and alignment by congruency interaction. One possible explanation would be that the face recognition in the extended system is more susceptible to attentional and cognitive control than regions in the “core” system because of their functional adjacency and connectivity to the cognitive control network. Another possibility is that, relative to rFFA and OFA, which process mainly perceptual inputs, the regions of the extended system per se are typically hubs of multiple functions. For instance, besides its role in face recognition, the precuneus is also a hub of the default mode network (Utevsky et al., 2014). Our results, from the perspective of the composite face effect, provide fresh evidence for the functional discrepancies between these two systems during face processing (Wang et al., 2017). However, the mechanisms underlying the differential participation between these two systems in holistic face processing requires further investigation.

4.4. The disproportional contribution of attentional, decisional and perceptual components

Moreover, we extended previous findings by quantitatively estimating the relative contribution of each component. Our results showed that the first dimension, probably attentional interference, accounts for over 86% of the behavioral variance in the composite face task. Meanwhile, the second dimension, probably response decision, accounts for another 4% - 10%. The percentages of variance accounted, together with significant neural-behavioral conformation in areas like the insula, medial frontal cortex and cingulate cortex, mirrors Paparello’s findings. Paparello (2007) found the most intense CFE occurred in frontal and parietal areas that are typically associated with working memory and spatial attention tasks, but not the temporo-occipital areas for percep-

tual face recognition. These observations suggest attentional and decisional operations are noticeably implicated in the outcomes of the composite face effect, at least when it is measured by the complete composite paradigm. However, our results do not mean that the low-level information is insignificant. Actually, the alignment effect in the right Cuneus, rFFA and rSTS suggested the involvement of the primary visual cortex and face network in the CFE effect. We interpreted these results as the orchestration of multiple cognitive operations behind the behavioral CFE effect. While it is meaningful to discern the perceptual relevance of in composite face effect, taking attentional and decisional operations into consideration in the CCP paradigm is also important in interpreting the outcome of the measurements. This may help reconcile the discrepancies in previous studies on face recognition, particularly those on the hotly-debated holistic face processing.

4.5. Limitations

Though the composite face effect provides one of the most compelling illustrations of holistic processing, the concept of holistic processing is multi-faceted and has been characterized by multiple tasks that may target different mechanisms (Li et al., 2017; Richler et al., 2012). The observations in the current study should be interpreted with caution as they do not necessarily generalize to other measurements of the holistic processing. Meanwhile, since the current study included only upright face materials, it is unclear if the cortical areas would be similarly involved in composite task of non-face materials or inverted faces. As reviewed in the introduction, the CFE effect has been reported in non-face stimuli (Bukach et al., 2010; Wong et al., 2009) and there are hot-debates about the “domain-specificity” and “domain-generality” of holistic processing (Gauthier and Bukach, 2007; McKone et al., 2013). Future work could explore the neural response patterns across face and non-face stimuli. Third, although decisional processes are not equal to motor commands (Richler and Gauthier, 2013), it is still interesting to investigate if cortices identified in the current study are still involved in tasks where participants match face parts covertly without a motor response, or in an experimental design where a motor response is required in only a small subset of trials and analysis of BOLD signal is restricted to the remaining trials with no overt response, which can help understand the relevant controversies (Richler and Gauthier, 2013; Rossion, 2013).

5. Conclusion

Our study demonstrates the involvement of both extended face processing and attention networks in the composite face effect (CFE), with most prominent neural-behavioral correspondence in distributed areas including the bilateral insula and medial frontal gyrus. These findings suggest the distinct contributions of face processing and attentional networks to the behavioral CFE outcome, and provide implications into face recognition and attentional control models for the CFE effect.

Declaration of Competing Interest

No conflicts in interests were declared.

Credit authorship contribution statement

Changming Chen: Conceptualization, Software, Formal analysis, Writing – original draft, Writing – review & editing. **Yixue Lou:** Data curation, Writing – review & editing. **Hong Li:** Conceptualization, Resources, Writing – review & editing. **Jiajin Yuan:** Conceptualization, Resources, Writing – review & editing. **Jiemin Yang:** Writing – review & editing. **Heather Winskel:** Writing – review & editing. **Shaozheng Qin:** Conceptualization, Resources, Writing – review & editing.

Acknowledgments

This work was supported by the National Natural Science Foundation of China (31871110, 32130045, 31971018, 81571056, 31671150, 31871103), the Natural Science Foundation of Henan Province (182300410366), Guangdong Key Project in “Development of new tools for diagnosis and treatment of Autism” (2018B030335001) and Humanities and Social Sciences Project of Education Department of Henan Province (2018-ZZJH-480). We thank genuinely the editor and reviewers for their constructive suggestions.

Data and code availability statement

Behavioral data, 3D datasets converted by the to3d program in AFNI, scripts for data analysis are available via https://osf.io/fsqaj.

Supplementary materials

Supplementary material associated with this article can be found, in the online version, at doi:10.1016/j.neuroimage.2021.118756.

References

Anderson, A.K., Christoff, K., Panitz, D., De Rosa, E., Gabrieli, J.D.E., 2003. Neural correlates of the automatic processing of threat facial signals. J. Neurosci. 23 (13), 5627. doi:10.1523/JNEUROSCI.23-13-05627.2003.

Andrews, T.J., Davies-Thompson, J., Kingstone, A., Young, A.W., 2010. Internal and external features of the face are represented holistically in face-selective regions of visual cortex. J. Neurosci. 30 (9), 3544–3552. doi:10.1523/JNEUROSCI.4863-09.2010.

Anzellotti, S., Fairhall, S.L., Caramazza, A., 2014. Decoding representations of face identity that are tolerant to rotation. Cereb. Cortex 24 (8), 1988–1995. doi:10.1093/cercor/bht046.

Arbula, S., Pisanu, E., Rumiati, R.I., 2021. Representation of social content in dorsomedial prefrontal cortex underlies individual differences in agreeableness trait. Neuroimage 235, 118049. doi:10.1016/j.neuroimage.2021.118049.

Ashby, F.G., Townsend, J.T., 1986. Varieties of perceptual independence. Psychol. Rev. 93 (2), 154–179.

Avidan, G., Tanzer, M., Behrmann, M., 2011. Impaired holistic processing in congenital prosopagnosia. Neuropsychologia 49 (9), 2541–2552. doi:10.1016/j.neuropsychologia.2011.05.002.

Avidan, G., Tanzer, M., Hadj-Bouziane, F., Liu, N., Ungerleider, L.G., Behrmann, M., 2014. Selective dissociation between core and extended regions of the face processing network in congenital prosopagnosia. Cereb. Cortex 24 (6), 1565–1578. doi:10.1093/cercor/bht007.

Axelrod, V., Yovel, G., 2010. External facial features modify the representation of internal facial features in the fusiform face area. Neuroimage 52 (2), 720–725. doi:10.1016/j.neuroimage.2010.04.027.

Benjaminsson, S., Fransson, P., Lansner, A., 2010. A novel model-free data analysis technique based on clustering in a mutual information space: application to resting-state fMRI. Front. Syst. Neurosci. 4 (34). doi:10.3389/fnsys.2010.00034.

Biotti, F., Wu, E., Yang, H., Jiahui, G., Duchaine, B., Cook, R., 2017. Normal composite face effects in developmental prosopagnosia. Cortex 95, 63–76. doi:10.1016/j.cortex.2017.07.018.

Botvinick, M.M., Braver, T.S., Barch, D.M., Carter, C.S., Cohen, J.D., 2001. Conflict monitoring and cognitive control. Psychol. Rev. 108 (3), 624–652. doi:10.1037/0033-295X.108.3.624.

Boutet, I., Gentes-Hawn, A., Chaudhuri, A., 2002. The influence of attention on holistic face encoding. Cognition 84 (3), 321–341. doi:10.1016/S0010-0277(02)00072-0.

Bukach, C.M., Phillips, W.S., Gauthier, I., 2010. Limits of generalization between categories and implications for theories of category specificity. Atten. Percept. Psychophys. 72 (7), 1865–1874. doi:10.3758/APP.72.7.1865.

Busigny, T., Joubert, S., Felician, O., Ceccaldi, M., Rossion, B., 2010. Holistic perception of the individual face is specific and necessary: evidence from an extensive case study of acquired prosopagnosia. Neuropsychologia 48 (14), 4057–4092. doi:10.1016/j.neuropsychologia.2010.09.017.

Busigny, T., Van Belle, G., Jemel, B., Hosein, A., Joubert, S., Rossion, B., 2014. Face-specific impairment in holistic perception following focal lesion of the right anterior temporal lobe. Neuropsychologia 56 (1), 312–333. doi:10.1016/j.neuropsychologia.2014.01.018.

Calder, A.J., Young, A.W., Keane, J., Dean, M., 2000. Configural information in facial expression perception. J. Exp. Psychol. Hum. Percept. Perform. 26 (2), 527–551. doi:10.1037//0096-1523.26.2.527.

Chen, C., Kao, K., Tyler, C., 2007. Face configuration processing in the human brain: the role of symmetry. Cereb. Cortex 17 (6), 1423–1432. doi:10.1093/cercor/bhl054.

Chen, C., Yang, J., Lai, J., Li, H., Yuan, J., Abbasi, N.u.H., 2015. Correlating gray matter volume with individual difference in the flanker interference effect. PLoS One 10 (8), e0136877. doi:10.1371/journal.pone.0136877.

Chen, W., Ren, N., Young, A.W., Liu, C., 2018. Interaction between social categories in the composite face paradigm. J. Exp. Psychol. Learn. Mem. Cogn. 44 (1), 34–49. doi:10.1037/xlm0000418.

Chua, K.W., Gauthier, I., 2020. Domain-specific experience determines individual differences in holistic processing. J. Exp. Psychol. Gen. 149 (1), 31–41. doi:10.1037/xge0000628.
Chua, K.W., Richler, J.J., Gauthier, I., 2014. Becoming a lunari or taiyo expert: learned attention to parts drives holistic processing of faces. J. Exp. Psychol. Hum. Percept. Perform. 40 (3), 1174–1182. doi:10.1037/a0035895.
Chua, K.W., Richler, J.J., Gauthier, I., 2015. Holistic processing from learned attention to parts. J. Exp. Psychol. Gen. 144 (4), 723–729. doi:10.1037/xge0000063.
Craig, A.D., 2009. How do you feel–now? The anterior insula and human awareness. Nat. Rev. Neurosci. 10 (1), 59–70. doi:10.1038/nrn2555.
Dailey, M.N., Cottrell, G.W., 1999. Organization of face and object recognition in modular neural network models. Neural Netw. 12 (7-8), 1053–1073. doi:10.1016/S0893-6080(99)00050-7.
DeGutis, J., Wilmer, J., Mercado, R.J., Cohan, S., 2013. Using regression to measure holistic face processing reveals a strong link with face recognition ability. Cognition 126 (1), 87–100. doi:10.1016/j.cognition.2012.09.004.
Dennett, H.W., McKone, E., Tavashmi, R., Hall, A., Pidcock, M., Edwards, M., Duchaine, B., 2012. The cambridge car memory test: a task matched in format to the cambridge face memory test, with norms, reliability, sex differences, dissociations from face memory, and expertise effects. Behav. Res. Methods 44 (2), 587–605. doi:10.3758/s13428-011-0160-2.
Eckert, M.A., Menon, V., Walczak, A., Ahlstrom, J., Denslow, S., Horwitz, A., Dubno, J.R., 2009. At the heart of the ventral attention system: the right anterior insula. Hum. Brain Mapp. 30 (8), 2530–2541. doi:10.1002/hbm.20688.
Eriksen, B.A., Eriksen, C.W., 1974. Effects of noise letters upon the identification of a target letter in a nonsearch task. Percept. Psychophy. 16 (1), 143–149. doi:10.3758/BF03203267.
Fan, J., 2014. An information theory account of cognitive control. Front. Hum. Neurosci. 8, 680. doi:10.3389/fnhum.2014.00680.
Fitousi, D., 2013. Mutual information, perceptual independence, and holistic face perception. Atten. Percept. Psychophys. 75 (5), 983–1000.
Fitousi, D., 2015. Composite faces are not processed holistically: evidence from the Garner and redundant target paradigms. Atten. Percept. Psychophys. 77 (6), 2037–2060. doi:10.3758/s13414-015-0887-4.
Fitousi, D., 2016. Comparing the role of selective and divided attention in the composite face effect: insights from attention operating characteristic (AOC) plots and cross-contingency correlations. Cognition 148, 34–46. doi:10.1016/j.cognition.2015.12.012.
Fitousi, D., 2020. Decomposing the composite face effect: evidence for non-holistic processing based on the ex-Gaussian distribution. Q. J. Exp. Psychol. 73 (6), 819–840. doi:10.1177/1747021820904222.
Fitousi, D., Algom, D., 2006. Size congruity effects with two-digit numbers: expanding the number line? Mem. Cognit. 34 (2), 445–457. doi:10.3758/bf03193421.
Foster, C., Bülthoff, I., Bartels, A., Zhao, M., 2021. Investigating holistic face processing within and outside of face-responsive brain regions. Neuroimage 226, 117565. doi:10.1016/j.neuroimage.2020.117565.
Foster, N.L., Dunlosky, J., Sahakyan, L., 2015. Is awareness of the ability to forget (or to remember) critical for demonstrating directed forgetting? J. Mem. Lang. 85, 88–100. doi:10.1016/j.jml.2015.06.009.
Gauthier, I., 2020. What we could learn about holistic face processing only from nonface objects. Curr. Dir. Psychol. Sci. 29 (4), 419–425. doi:10.1177/0963721420920620.
Gauthier, I., Bukach, C.M., 2007. Should we reject the expertise hypothesis? Cognition 103 (2), 322–330. doi:10.1016/j.cognition.2006.05.003.
Gauthier, I., Klaiman, C., Schultz, R.T., 2009. Face composite effects reveal abnormal face processing in autism spectrum disorders. Vis. Res. 49 (4), 470–478. doi:10.1016/j.visres.2008.12.007.
Gauthier, I., Skudlarski, P., Gore, J.C., Anderson, A.W., 2000. Expertise for cars and birds recruits brain areas involved in face recognition. Nat. Neurosci. 3 (2), 191–197. doi:10.1038/72140.
Gauthier, I., Tarr, M.J., 1997. Becoming a “greeble” expert: exploring mechanisms for face recognition. Vis. Res. 37 (12), 1673–1682. doi:10.1016/S0042-6989(96)00286-6.
Gauthier, I., Tarr, M.J., 2002. Unraveling mechanisms for expert object recognition: bridging brain activity and behavior. J. Exp. Psychol. Hum. Percept. Perform. 28 (2), 431–446. doi:10.1037//0096-1523.28.2.431.
Gauthier, I., Williams, P., Tarr, M.J., Tanaka, J., 1998. Training ’greeble’ experts: a framework for studying expert object recognition processes. Vis. Res. 38 (15-16), 2401–2428. doi:10.1016/S0042-6989(97)00442-2.
Gobbini, M.I., Haxby, J.V., 2006. Neural response to the visual familiarity of faces. Brain Res. Bull. 71 (1), 76–82. doi:10.1016/j.brainresbull.2006.08.003.
Goffaux, V., Schiltz, C., Mur, M., Goebel, R., 2013. Local discriminability determines the strength of holistic processing for faces in the fusiform face area. Front. Psychol. 3 (604). doi:10.3389/fpsyg.2012.00604.
Grand, R.L., Mondloch, C.J., Maurer, D., Brent, H.P., 2004. Impairment in holistic face processing following early visual deprivation. Psychol. Sci. 15 (11), 762–768. doi:10.1111/j.0956-7976.2004.00753.x.
Harris, A., Aguirre, G.K., 2008. The representation of parts and wholes in face-selective cortex. J. Cogn. Neurosci. 20 (5), 863–878. doi:10.1162/jocn.2008.20509.
Harris, A., Aguirre, G.K., 2010. Neural tuning for face wholes and parts in human fusiform gyrus revealed by FMRI adaptation. J. Neurophysiol. 104 (1), 336–345. doi:10.1152/jn.00626.2009.
Hole, G.J., 1994. Configurational factors in the perception of unfamiliar faces. Perception 23 (1), 65–74. doi:10.1068/p230065.
Huang, Z., Tarnal, V., Vlisides, P.E., Janke, E.L., McKinney, A.M., Picton, P., Hudetz, A.G., 2021. Anterior insula regulates brain network transitions that gate conscious access. Cell Rep. 35 (5), 109081. doi:10.1016/j.celrep.2021.109081.
Jacques, C., Rossion, B., 2009. The initial representation of individual faces in the right occipito-temporal cortex is holistic: electrophysiological evidence from the composite face illusion. J. Vis. 9 (6). doi:10.1167/9.6.8.
Kamps, F.S., Morris, E.J., Dilks, D.D., 2019. A face is more than just the eyes, nose, and mouth: fMRI evidence that face-selective cortex represents external features. Neuroimage 184, 90–100. doi:10.1016/j.neuroimage.2018.09.027.
Klumpp, H., Post, D., Angstadt, M., Fitzgerald, D.A., Phan, K.L., 2013. Anterior cingulate cortex and insula response during indirect and direct processing of emotional faces in generalized social anxiety disorder. Biol. Mood Anxiety Disord. 3 (1), 7. doi:10.1186/2045-5380-3-7.
Konar, Y., Bennett, P.J., Sekuler, A.B., 2010. Holistic processing is not correlated with face-identification accuracy. Psychol. Sci. 21 (1), 38–43. doi:10.1177/0956797609356508.
Kriegeskorte, N., Goebel, R., Bandettini, P., 2006. Information-based functional brain mapping. Proc. Natl. Acad. Sci. U. S. A. 103 (10), 3863–3868. doi:10.1073/pnas.0600244103.
Kriegeskorte, N., Mur, M., Bandettini, P., 2008. Representational similarity analysis - connecting the branches of systems neuroscience. Front. Syst. Neurosci. 2 (4). doi:10.3389/neuro.06.004.2008.
Kriegeskorte, N., Mur, M., Ruff, D.A., Kiani, R., Bodurka, J., Esteky, H., Bandettini, P.A., 2008. Matching categorical object representations in inferior temporal cortex of man and monkey. Neuron 60 (6), 1126–1141. doi:10.1016/j.neuron.2008.10.043.
Kuefner, D., Jacques, C., Prieto, E.A., Rossion, B., 2010. Electrophysiological correlates of the composite face illusion: disentangling perceptual and decisional components of holistic face processing in the human brain. Brain Cogn. 74 (3), 225–238. doi:10.1016/j.bandc.2010.08.001.
Le Grand, R., Cooper, P., Mondloch, C., Lewis, T., Sagiv, N., Gelder, B., Maurer, D., 2006. What aspects of face processing are impaired in developmental prosopagnosia? Brain Cogn. 61, 139–158. doi:10.1016/j.bandc.2005.11.005.
Lee, Y., Anaki, D., Grady, C.L., Moscovitch, M., 2012. Neural correlates of temporal integration in face recognition: an fMRI study. Neuroimage 61 (4), 1287–1299. doi:10.1016/j.neuroimage.2012.02.073.
Levine, S.M., Schwarzbach, J.V., 2021. Individualizing representational similarity analysis. Front. Psychiatry 12 (1727). doi:10.3389/fpsyt.2021.729457.
Li, J., Huang, L., Song, Y., Liu, J., 2017. Dissociated neural basis of two behavioral hallmarks of holistic face processing: the whole-part effect and composite-face effect. Neuropsychologia 102, 52–60. doi:10.1016/j.neuropsychologia.2017.05.026.
Liu, C.H., Young, A.W., Basra, G., Ren, N., Chen, W., 2020. Perceptual integration and the composite face effect. Q. J. Exp. Psychol. 73 (7), 1101–1114. doi:10.1177/1747021819899531, (Hove).
Liu, J., Harris, A., Kanwisher, N., 2010. Perception of face parts and face configurations: an fMRI study. J. Cogn. Neurosci. 22 (1), 203–211. doi:10.1162/jocn.2009.21203.
Liu, T.T., Behrmann, M., 2014. Impaired holistic processing of left-right composite faces in congenital prosopagnosia. Front. Hum. Neurosci. 8, 750. doi:10.3389/fnhum.2014.00750.
Margulies, D.S., Vincent, J.L., Kelly, C., Lohmann, G., Uddin, L.Q., Biswal, B.B., Petrides, M., 2009. Precuneus shares intrinsic functional architecture in humans and monkeys. Proc. Natl. Acad. Sci. 106 (47), 20069–20074. doi:10.1073/pnas.0905314106.
Maurer, D., Grand, R.L., Mondloch, C.J., 2002. The many faces of configural processing. Trends Cogn. Sci. 6 (6), 255–260. doi:10.1016/S1364-6613(02)01903-4.
Maurer, D., O’Craven, K., Grand, R.L., Mondloch, C., Springer, M., Lewis, T., Grady, C., 2007. Neural correlates of processing facial identity based on features versus their spacing. Neuropsychologia 45, 1438–1451.
McKone, E., Aimola Davies, A., Darke, H., Crookes, K., Wickramariyaratne, T., Zappia, S., Fernando, D., 2013. Importance of the inverted control in measuring holistic face processing with the composite effect and part-whole effect. Front. Psychol. 33. doi:10.3389/fpsyg.2013.00033.
McKone, E., Stokes, S., Liu, J., Cohan, S., Fiorentini, C., Pidcock, M., Pelleg, M., 2012. A robust method of measuring other-race and other-ethnicity effects: the cambridge face memory test format. PLoS One 7 (10), e47956. doi:10.1371/journal.pone.0047956.
Menon, V., Gallardo, G., Pinsk, M.A., Nguyen, V.D., Li, J.R., Cai, W., Wassermann, D., 2020. Microstructural organization of human insula is linked to its macrofunctional circuitry and predicts cognitive control. Elife 9. doi:10.7554/eLife.53470.
Menon, V., Uddin, L.Q., 2010. Saliency, switching, attention and control: a network model of insula function. Brain Struct. Funct. 214, 655–667. doi:10.1007/s00429-010-0262-0.
Murphy, J., Gray, K.L.H., Cook, R., 2017. The composite face illusion. Psychon. Bull. Rev. 24 (2), 245–261. doi:10.3758/s13423-016-1131-5.
Nagahama, Y., Okada, T., Katsumi, Y., Hayashi, T., Yamauchi, H., Sawamoto, N., Shibasaki, H., 1999. Transient neural activity in the medial superior frontal gyrus and precuneus time locked with attention shift between object features. Neuroimage 10 (2), 193–199. doi:10.1006/nimg.1999.0451.
Nasr, S., Tootell, R.B.H., 2012. Role of fusiform and anterior temporal cortical areas in facial recognition. Neuroimage 63 (3), 1743–1753. doi:10.1016/j.neuroimage.2012.08.031.
Nee, D.E., Wager, T.D., Jonides, J., 2007. Interference resolution: insights from a meta-analysis of neuroimaging tasks. Cogn. Affect. Behav. Neurosci. 7 (1), 1–17. doi:10.3758/CABN.7.1.1.
Paparello, S., 2007. The Many Faces of Neurocognitive Development: Behavior and Neurocorrelates of Holistic Face Processing: Behavior and Neurocorrelates of Holistic Face Processing. University of California, San Diego (Doctor).
Popal, H., Wang, Y., Olson, I., 2020. A guide to representational similarity analysis for social neuroscience. Soc. Cogn. Affect. Neurosci. 14. doi:10.1093/scan/nsz099.
Qin, S., Cho, S., Chen, T., Rosenberg-Lee, M., Geary, D.C., Menon, V., 2014. Hippocampal-neocortical functional reorganization underlies children’s cognitive development. Nat. Neurosci. 17 (9), 1263–1269. doi:10.1038/NN.3788.

Qin, S., Young, C.B., Duan, X., Chen, T., Supekar, K., Menon, V., 2014. Amygdala subregional structure and intrinsic functional connectivity predicts individual differences in anxiety during early childhood. Biol. Psychiatry 75 (11), 892–900. doi:10.1016/j.biopsych.2013.10.006.

Ramon, M., Busigny, T., Rossion, B., 2010. Impaired holistic processing of unfamiliar individual faces in acquired prosopagnosia. Neuropsychologia 48 (4), 933–944. doi:10.1016/j.neuropsychologia.2009.11.014.

Renzi, C., Schiavi, S., Carbon, C., Vecchi, T., Silvanto, J., Cattaneo, Z., 2013. Processing of featural and configural aspects of faces is lateralized in dorsolateral prefrontal cortex: a TMS study. Neuroimage 74, 45–51. doi:10.1016/j.neuroimage.2013.02.015.

Rezlescu, C., Susilo, T., Wilmer, J.B., Caramazza, A., 2017. The inversion, part-whole, and composite effects reflect distinct perceptual mechanisms with varied relationships to face recognition. J. Exp. Psychol. Hum. Percept. Perform. 43 (12), 1961–1973. doi:10.1037/xhp0000400.

Richler, J.J., Cheung, O.S., Gauthier, I., 2011. Holistic processing predicts face recognition. Psychol. Sci. 22 (4), 464–471. doi:10.1177/0956797611401753.

Richler, J.J., Cheung, O.S., Wong, A.C., Gauthier, I., 2009. Does response interference contribute to face composite effects? Psychon. Bull. Rev. 16 (2), 258–263. doi:10.3758/PBR.16.2.258.

Richler, J.J., Gauthier, I., 2013. When intuition fails to align with data: a reply to Rossion (2013). Vis. Cogn. 21 (2). doi:10.1080/13506285.2013.796035.

Richler, J.J., Gauthier, I., Wenger, M.J., Palmeri, T.J., 2008. Holistic processing of faces: perceptual and decisional components. J. Exp. Psychol. Learn. Mem. Cogn. 34 (2), 328–342. doi:10.1037/0278-7393.34.2.328.

Richler, J.J., Palmeri, T.J., Gauthier, I., 2012. Meanings, mechanisms, and measures of holistic processing. Front. Psychol. 3 (DEC). doi:10.3389/fpsyg.2012.00553.

Ross, D.A., Tamber-Rosenau, B.J., Palmeri, T.J., Zhang, J., Xu, Y., Gauthier, I., 2018. High-resolution functional magnetic resonance imaging reveals configural processing of cars in right anterior fusiform face area of car experts. J. Cogn. Neurosci. 30 (7), 973–984. doi:10.1162/jocn_a_01256.

Rossion, B., 2013. The composite face illusion: a whole window into our understanding of holistic face perception. Vis. Cogn. 21 (2), 139–253. doi:10.1080/13506285.2013.772929.

Rotshtein, P., Geng, J.J., Driver, J., Dolan, R.J., 2007. Role of features and second-order spatial relations in face discrimination, face recognition, and individual face skills: behavioral and functional magnetic resonance imaging data. J. Cogn. Neurosci. 19 (9), 1435–1452. doi:10.1162/jocn.2007.19.9.1435.

Schiltz, C., Dricot, L., Goebel, R., Rossion, B., 2010. Holistic perception of individual faces in the right middle fusiform gyrus as evidenced by the composite face illusion. J. Vis. 10 (2), 1–16. doi:10.1167/10.2.25.

Schiltz, C., Rossion, B., 2006. Faces are represented holistically in the human occipito-temporal cortex. Neuroimage 32 (3), 1385–1394. doi:10.1016/j.neuroimage.2006.05.037.

Soria Bauser, D.A., Suchan, B., Daum, I., 2011. Differences between perception of human faces and body shapes: evidence from the composite illusion. Vis. Res. 51 (1), 195–202. doi:10.1016/j.visres.2010.11.007.

Stanislaw, H., Todorov, N., 1999. Calculation of signal detection theory measures. Behav. Res. Methods Instrum. Comput. 31 (1), 137–149. doi:10.3758/bf03207704.

Susilo, T., McKone, E., Dennett, H., Darke, H., Palermo, R., Hall, A., Rhodes, G., 2010. Face recognition impairments despite normal holistic processing and face space coding: evidence from a case of developmental prosopagnosia. Cogn. Neuropsychol. 27 (8), 636–664. doi:10.1080/02643294.2011.613372.

Susilo, T., Rezlescu, C., Duchaine, B., 2013. The composite effect for inverted faces is reliable at large sample sizes and requires the basic face configuration. J. Vis. 13 (13), 14. doi:10.1167/13.13.14, -14.

Talati, A., Hirsch, J., 2005. Functional specialization within the medial frontal gyrus for perceptual go/no-go decisions based on "what," "when," and "where" related information: an fMRI study. J. Cogn. Neurosci. 17 (7), 981–993. doi:10.1162/0898929054475226.

Tanaka, J.W., Farah, M.J., 1993. Parts and wholes in face recognition. Q. J. Exp. Psychol. Sect. A 46 (2), 225–245. doi:10.1080/14640749308401045.

Tanaka, J.W., Simonyi, D., 2016. The "parts and wholes" of face recognition: a review of the literature. Q. J. Exp. Psychol. 69 (10), 1876–1889. doi:10.1080/17470218.2016.1146780, (2006).

Todorov, A., Loehr, V., Oosterhof, N.N., 2010. The obligatory nature of holistic processing of faces in social judgments. Perception 39 (4), 514–532. doi:10.1068/p6501.

Tso, R.V., Chen, H., Yeung, Y.A., Au, T., Hsiao, J., 2017. Right hemisphere lateralization and holistic processing do not always go together: an ERP investigation of a training study. Cogn. Sci. 3386–3391.

Tzagarakis, C., Jerde, T.A., Lewis, S.M., Uğurbil, K., Georgopoulos, A.P., 2009. Cerebral cortical mechanisms of copying geometrical shapes: a multidimensional scaling analysis of fMRI patterns of activation. Exp. Brain Res. 194 (3), 369–380. doi:10.1007/s00221-009-1709-5.

Uddin, L.Q., Nomi, J.S., Hébert-Seropian, B., Ghaziri, J., Boucher, O., 2017. Structure and function of the human insula. J. Clin. Neurophysiol. 34 (4), 300–306. doi:10.1097/wnp.0000000000000377.

Ullsperger, M., Harsay, H.A., Wessel, J.R., Ridderinkhof, K.R., 2010. Conscious perception of errors and its relation to the anterior insula. Brain Struct. Funct. 214 (5), 629–643. doi:10.1007/s00429-010-0261-1.

Utevsky, A.V., Smith, D.V., Huettel, S.A., 2014. Precuneus is a functional core of the default-mode network. J. Neurosci. 34 (3), 932–940. doi:10.1523/jneurosci.4227-13.2014.

Varoquaux, G., 2018. Cross-validation failure: small sample sizes lead to large error bars. Neuroimage 180, 68–77. doi:10.1016/j.neuroimage.2017.06.061.

Ventura, P., Leite, I., Fernandes, T., 2018. The development of holistic face processing: an evaluation with the complete design of the composite task. Acta Psychol. (Amst) 191, 32–41. doi:10.1016/j.actpsy.2018.08.015.

Von Der Heide, R.J., Wenger, M.J., Bittner, J.L., Fitousi, D., 2018. Converging operations and the role of perceptual and decisional influences on the perception of faces: neural and behavioral evidence. Brain Cogn. 122 (October 2017), 59–75. doi:10.1016/j.bandc.2018.01.007.

Walther, A., Nili, H., Ejaz, N., Alink, A., Kriegeskorte, N., Diedrichsen, J., 2016. Reliability of dissimilarity measures for multi-voxel pattern analysis. Neuroimage 137, 188–200. doi:10.1016/J.NEUROIMAGE.2015.12.012.

Wang, R., Li, J., Fang, H., Tian, M., Liu, J., 2012. Individual differences in holistic processing predict face recognition ability. Psychol. Sci. 23 (2), 169–177. doi:10.1177/0956797611420575.

Wang, X., Zhu, Q., Song, Y., Liu, J., 2017. Developmental reorganization of the core and extended face networks revealed by global functional connectivity. Cereb. Cortex 28 (10), 3521–3530. doi:10.1093/cercor/bhx217.

Wang, Y., Guo, S., Sun, Q., Jin, S.F., Zhang, X., Xiao, M., Li, K.Z., 2019. Anthropometric labial analysis of Han Chinese young adults. Skin Res. Technol. 25 (4), 499–503. doi:10.1111/srt.12678.

Wong, A.C., Bukach, C.M., Hsiao, J., Greenspon, E., Ahern, E., Duan, Y., Lui, K.F., 2012. Holistic processing as a hallmark of perceptual expertise for nonface categories including Chinese characters. J. Vis. 12 (13), 7. doi:10.1167/12.13.7.

Wong, A.C., Palmeri, T.J., Rogers, B.P., Gore, J.C., Gauthier, I., 2009. Beyond shape: how you learn about objects affects how they are represented in visual cortex. PLoS One 4 (12). doi:10.1371/journal.pone.0008405.

Wu, T., Schulz, K.P., Fan, J., 2021. Activation of the cognitive control network associated with information uncertainty. Neuroimage 230, 117703. doi:10.1016/j.neuroimage.2020.117703.

Wu, T., Spagna, A., Chen, C., Schulz, K.P., Hof, P.R., Fan, J., 2020. Supramodal mechanisms of the cognitive control network in uncertainty processing. Cereb. Cortex 30 (12), 6336–6349. doi:10.1093/cercor/bhaa189.

Wu, T., Wang, X., Wu, Q., Spagna, A., Yang, J., Yuan, C., Fan, J., 2019. Anterior insular cortex is a bottleneck of cognitive control. Neuroimage 195, 490–504. doi:10.1016/j.neuroimage.2019.02.042.

Xie, W., Zhang, W., 2016. The influence of emotion on face processing. Cogn. Emot 30 (2), 245–257. doi:10.1080/02699931.2014.994477.

Yang, L.Z., Zhang, W., Shi, B., Yang, Z., Wei, Z., Gu, F., Rao, H., 2014. Electrical stimulation over bilateral occipito-temporal regions reduces N170 in the right hemisphere and the composite face effect. PLoS One 9 (12). doi:10.1371/journal.pone.0115772.

Yin, R.K., 1969. Looking at upside-down faces. J. Exp. Psychol. 81 (1), 141–145. doi:10.1037/H0027474.

Young, A.W., Hellawell, D., Hay, D.C., 1987. Configurational information in face perception. Perception 16 (6), 747–759. doi:10.1068/p160747.

Zhang, H., Tian, J., Liu, J., Li, J., Lee, K., 2009. Intrinsically organized network for face perception during the resting state. Neurosci. Lett. 454 (1), 1–5. doi:10.1016/j.neulet.2009.02.054.

Zhang, J., Liu, J., Xu, Y., 2015. Neural decoding reveals impaired face configural processing in the right fusiform face area of individuals with developmental prosopagnosia. J. Neurosci. 35 (4), 1539–1548. doi:10.1523/jneurosci.2646-14.2015.

Zhao, M., Bülthoff, H.H., Bülthoff, I., 2015. Beyond faces and expertise: facelike holistic processing of nonface objects in the absence of expertise. Psychol. Sci. 27 (2), 213–222. doi:10.1177/0956797615617779.

Zhao, M., Bülthoff, H.H., Bülthoff, I., 2016. A shape-based account for holistic face processing. J. Exp. Psychol. Learn. Mem. Cogn. 42 (4), 584–597. doi:10.1037/xlm0000185.

Zhao, M., Hayward, W.G., Bülthoff, I., 2014. Holistic processing, contact, and the other-race effect in face recognition. Vis. Res. 105, 61–69. doi:10.1016/j.visres.2014.09.006.